

TEMPERATURE AND VELOCITY DISTRIBUTION  
IN THE WAKE OF A HEATED CYLINDER

Thesis by

David Malcolm Mason, Jr.

In Partial Fulfillment of the Requirements

For the Degree of

Doctor of Philosophy

California Institute of Technology

Pasadena, California

1949

## Acknowledgment

The experimental data presented in this thesis were obtained through the joint efforts of graduate students of the Chemical Engineering Laboratory at the California Institute of Technology. Great credit is due G. W. Billman and W. H. Corcoran for their untiring efforts in the design and construction of the equipment used in this investigation. S. D. Cavers, J. L. Mason, and F. Page, Jr. contributed generously of their time in both the experimental work and the processing of the data, and their cooperation is gratefully appreciated. Financial support for the program was obtained from the Institute through the effort of Dr. B. H. Sage who planned and initiated the over-all research program. The technical guidance of both Dr. Sage and Dr. W. N. Lacey helped materially in the successful prosecution of the experimental work. In the construction and operation of equipment the aid of Institute employees such as D. K. Breaux, W. M. DeWitt, G. A. Griffith, and H. H. Reamer was indispensable. Special thanks are due Carol Brewster, Audrey Downer, and Shirley Scheele for the typing of the manuscript, and Anne Jarvis for the preparation of the figures.

## Abstract

Detailed measurements of the temperature and velocity distribution in the two-dimensional wake of a heated cylinder are presented. Measurements of the temperature distribution on the surface of the cylinder for various rates of heat dissipation are also included, and these data are correlated in the form of dimensionless parameters. The cylinder was 12.15 inches long and 0.190 inch in outside diameter and was placed midway between the upper and lower parallel walls of a horizontal conduit of rectangular cross section through which air flowed normal to the cylinder. The walls, which were spaced 0.75 inch apart, were independently maintained at desired temperatures. In one series of measurements of the temperature and velocity distribution in the wake the rate of heat dissipation from the cylinder was maintained at a constant value of 5.42 watts per inch length of the cylinder for Reynolds numbers of 4,270, 7,630, 15,200, and 26,900 based on the free cross-section area of the conduit. In another series of measurements at a Reynolds number of 15,200 the rate of heat dissipation from the cylinder was maintained at 1.70 watts per inch and 3.20 watts per inch. In each of the above cases the temperature of the walls of the conduit was maintained at 100°F, identical to the bulk temperature of the entering air. In addition measurements at a Reynolds number of 15,200 were made with the entering air at a temperature of 100°F, the upper wall at 130°F,

the lower wall at  $70^{\circ}\text{F}$ , and a rate heat dissipation of about 5.43 watts per inch. Point values of temperature and velocity were obtained as a function of position in the wake of the cylinder. From these data values of eddy conductivity and eddy viscosity were calculated. Analysis of the data on the basis of Prandtl's momentum transfer theory and Taylor's vorticity transfer theory is included. The results are given in tabular form, and a number of graphical presentations of the data are included.

## TABLE OF CONTENTS

<u>PART</u>	<u>TITLE</u>	<u>PAGE</u>
I.	Introduction . . . . .	1
II.	Description of Equipment . . . . .	6
III.	Experimental Methods and Sources of Error . . . . .	11
IV.	Experimental Results . . . . .	17
V.	Theoretical Analysis of Results . . . . .	27
VI.	Conclusions . . . . .	42
VII.	Nomenclature . . . . .	44
VIII.	References . . . . .	48
IX.	Figures . . . . .	50
X.	Tables . . . . .	76

## Introduction

The Chemical Engineering Laboratory of the California Institute of Technology has undertaken an investigation of the fundamental mechanism of transfers of momentum, heat, and material in a turbulently flowing air stream. The experimental results on the temperature and velocity distribution in the wake of a heated cylinder presented herein represent but a part of the overall transfer research program. The nature of the whole program will be briefly outlined as a means of presenting in perspective the relationship between the heated cylinder work and the other investigations of transfers in turbulent air streams. The investigations were carried out in a wind tunnel of rectangular cross section through which air flowed at a desired bulk velocity.

One phase of the program involved an investigation of momentum, heat, and material transfers in a turbulently flowing air stream when no obstacle was in the channel. The random motion of particles of the fluid in turbulent flow is manifested in fluctuating components of velocity, and the instantaneous velocities  $u$  and  $v$  in two-dimensional flow can be described in terms of the time average flow whose components are  $\bar{u}$  and  $\bar{v}$ , and the superposed turbulent fluctuations whose components are  $u'$  and  $v'$ , the time average values of which are zero (upper portion of Figure 1).  $u$  is the velocity in the longitudinal or  $x$ -direction;  $v$  is the velocity in the vertical or  $y$ -direction. For two dimensional flow between parallel plates,  $s$ , the velocity in the lateral or  $z$ -direction is zero. Explanation of the nomenclature used is given on page 44. The interaction of the fluctuating velocities causes an

interchange of momentum with the development of a corresponding tangential shearing stress. Thus, superposed upon the tangential stress due to viscous sliding of adjacent fluid layers over one another is the stress due to the turbulent agent, and the aggregate stress can be expressed by the differential equation for momentum transfer (1):

$$\tau_{yx} = K_1(\epsilon_{my} + \nu) \frac{du}{dy} \quad (1)$$

The term  $\epsilon_{my}$ , the eddy viscosity, represents the forces arising from turbulence; whereas,  $\nu$ , the kinematic viscosity represents the molecular viscous forces. Similarly for the transfer of heat to the flowing stream from the upper wall of the conduit:

$$\frac{\dot{Q}}{C_p \sigma} = K_2(\epsilon_{cy} + \kappa) \frac{dt}{dy} \quad (2)$$

$\epsilon_{cy}$  is the eddy conductivity arising from turbulence, and  $\kappa$  is the thermometric conductivity for molecular conduction of heat. For the evaporation of a volatile material from the lower wall of the conduit into the gas stream (Figure 1)

$$M = K_3(\epsilon_{dy} + D) \frac{dc}{dy} \quad (3)$$

$E_{dy}$ , is the eddy diffusivity arising from turbulence, and  $D$  is the molecular diffusivity.

There exists a relationship between the manner in which momentum, heat, and material are transferred in turbulent fluids. Reynolds in 1874 suggested the fact that the various modes of transfer occur in an analogous manner (2). As a consequence of Reynolds analogy, the eddy quantities  $E_c$ ,  $E_m$ , and  $E_d$  should be equal in turbulently flowing gas streams (3). To what degree the Reynolds analogy applies under various conditions of turbulent flow remains to be found from precise experimental data.

In the investigation of two-dimensional flow with no obstacle in the channel, the values of the eddy quantities can be accurately determined from Equations (1), (2), and (3). In these equations all physical quantities beside the eddy quantities are either experimentally determined or are known properties of the fluid. By Equation (1)  $E_{my}$  is derived from measurements of point velocity in the  $y$ -direction,  $\bar{v}_{yx}$  being determined from static pressure measurements along the channel, and  $\mathcal{V}$  being a property of the air. By Equation (2)  $E_{ay}$  is determined from measurements of the temperature distribution in the channel and the rate of heat transferred to the air per unit area of the wall (Figure 1).  $C_p$ ,  $\sigma$ , and  $K$  are properties of the medium. By Equation (3)  $E_p$  is determined from the measurement of the concentration distribution in the channel and the rate of transfer of material into the gas stream.  $D$  is the property of the gas. Thus for the simple case of uniformly developed turbulent flow in the channel these eddy quantities can be



readily determined experimentally.

Of interest to the chemical engineer is the investigation of transfer of momentum and heat in the wake of obstacles of various shapes. This investigation represents another phase of the transfer research program. The investigations in the wake of obstacles of various shapes were initiated with the measurements of the temperature and velocity distribution in the wake of a heated cylinder presented herein. Incomplete data on the velocity distribution in the wake of an unheated cylinder and temperature distribution in the wake of a heated cylinder are available in the literature (4,5,6,7,8). However, no thorough investigation of the temperature and velocity distribution in the wake of a heated cylinder has been made at various distances downstream of the cylinder and for various Reynolds numbers and rates of heat dissipation. The temperature and velocity data of the present investigation are discussed primarily from a qualitative point of view. Equations derived subsequently are used with simplifying assumptions to calculate values of  $\epsilon_c$  and  $\epsilon_m$  from the temperature and velocity distribution data (Figure 1). The Reynolds analogy is tested by a comparison of the ratio of the eddy quantities to the theoretical ratio of unity.

Prandtl's momentum transfer theory and Taylor's vorticity transport theory (9) present ideas as to the mechanism of turbulence and provide the engineer with convenient equations for predicting the temperature and velocity distribution in turbulently flowing streams. The validity of these contrasting theories can

be tested by means of the heated cylinder data.

Whereas the eddy quantities are point concepts, the idea of over-all transfer coefficients represented by the heat transfer coefficient and friction factor is the most powerful tool presently at the disposal of the engineer. Data are included as to the over-all heat transfer coefficient from the cylinder as a function of Reynolds number.

In the present measurements point values of temperature and velocity were determined in a substantially two-dimensional air stream in the wake of a heated cylinder. The cylinder was located midway between the walls of the channel, normal to the flow, and temperatures and velocities were determined at a large number of points downstream of the cylinder in a vertical plane intersecting the longitudinal mid-line of the cylinder. In this plane vertical temperature and velocity traverses between the walls were made at frequent intervals downstream from the cylinder so as to show the temperature and velocity distribution in detail.

The temperature and velocity distribution studies were carried out for bulk air velocities of 6.99, 12.7, 24.8, and 44.7 feet per second, which correspond to Reynolds numbers of 4,270, 7,630, 15,200, and 26,900 based on the free cross-section area of the flow channel or 562, 1,221, 2,285, and 4,440 based on the outside diameter of the cylinder. The temperature of the walls of the conduit and the bulk temperature of the inlet air were maintained at 100°F. In addition one set of measurements at a Reynolds number of 15,200 was made in the wake with the upper wall at 130°F, the lower wall at 70°F, and the entering air at 100°F. A rate of heat dissipation

from the cylinder of 4,460 B.t.u. per hour per square foot corresponding to 5.42 watts per inch length of the cylinder was maintained at each Reynolds number in the above measurements. In addition, for a Reynolds number of 15,200 the temperature and velocity distribution were determined for rates of heat dissipation of 1.70 watts per inch and 3.20 watts per inch.

At each of the above Reynolds numbers the rate of heat dissipation was varied over a wide range and the average surface temperature of the cylinder was measured as a function of these rates. At bulk air velocities of 14.4 and 23.8 feet per second, which correspond to Reynolds numbers of 1,160 and 1,920 based on the cylinder diameter, the circumferential temperature distribution on the surface of the cylinder at its longitudinal midline was measured for several values of heat dissipation.

#### Description of Equipment

The equipment consisted essentially of a closed horizontal flow channel 13 feet in length of rectangular cross section, 0.75 inch in height, and 12 inches in width. The apparatus is described thoroughly elsewhere (10,11), so that only the most general features of the equipment will be discussed herein. The general arrangement of the equipment is shown in Figure 2. Air was supplied to the channel A at the desired bulk velocity by means of blower B. The temperature of the upper and lower plates which comprised the top and bottom of the conduit, was maintained at a predetermined value by means of oil rapidly circulating in baths C external to the plates. The temperature of the oil in each bath and the bulk inlet air

temperature were controlled by appropriate electronic circuits. Suitable traversing equipment was employed to permit the careful location of the instruments which measured the point temperature and velocity in the wake of the heated cylinder.

The cylinder used in most of the measurements consisted of a stainless steel tube 0.190 inch in outside diameter and 0.170 inch in inside diameter. The tube itself was used as the heater element for the conversion of electrical energy into heat. The cylinder was located midway between the walls normal to the direction of flow, 6 feet from the entrance to the conduit. In Figure 3 the steel cylinder is shown positioned in the channel. In an insert to this figure the details of construction of the cylinder are shown. In order that the rate of heat dissipation per unit length of the cylinder in the region near the lateral midline of the channel could be determined independently of the nonuniform dissipation near the ends of the cylinder, potential leads were connected to contact rings located on the interior of the tube as indicated at A and B. These rings were soldered to the inside of the tube, and the distance between them was carefully established. From a measurement of the current flowing through the cylinder and the potential difference between the contact rings it was possible to establish the rate of heat transferred per unit length of the tube. The electrical resistance of the cylinder was determined as a function of temperature when the cylinder was maintained in an isothermal bath at a series of known temperatures. To determine the resistance of the cylinder the potential between the contact rings was measured for known, small values of current flowing through the cylinder.

The steel cylinder was employed in all measurements of temperature and velocity in the wake.

A brass cylinder of the same over-all dimensions as the steel cylinder was used for the estimation of the circumferential distribution of surface temperature at the longitudinal midline of the cylinder. The cylinder consisted of a brass tube split longitudinally. A nichrome wire heater was placed inside, and copper constantan thermocouples were imbedded in the walls of the tube. The brass cylinder is shown situated in the channel in Figure 4, and in the insert to this figure are shown the details of assembly of the thermocouples and the internal heater in the brass tube. Potential leads for the determination of the rate of energy addition to the heater were connected to the nichrome heater element. An estimate of the circumferential variation in surface temperature for various rates of heat dissipation was obtained by means of the thermocouples.

Each thermocouple was placed in a small hole drilled radially in the surface of the cylinder. Six holes equally spaced about the circumference were drilled in the middle of the cylinder. Eight other thermocouples were located lengthwise along the cylinder for a check of the longitudinal uniformity of temperature on the cylinder. The hot junction of each thermocouple was located as nearly flush with the outside surface of the cylinder as possible and was insulated from the adjacent metal by a small layer of bakelite cement. The physical disposition of the thermocouples made it doubtful whether or not the actual surface temperature of the cylinder was measured.

An instrument, which will hereafter be referred to as a therm-anemometer was used to measure point values of temperature and velocity.

The thermanemometer, which consisted of a 0.5-mil platinum wire, together with a pitot tube, was suspended in the air stream by means of two piano wires as shown in Figure 5. These piano wires in turn were rigidly connected to the traversing equipment which enabled longitudinal and vertical movement of the thermanemometer in the wake. The 0.5-mil platinum wire suspended normal to the flowing air stream on two platinum needles was used to measure the temperature and velocity at a point in the air stream. Since flow was essentially two dimensional there was no temperature or velocity gradient along the wire, and therefore because of its small diameter, the wire was capable of measuring essentially point values of temperature and velocity. Current flowed through the wire when it was used as a hot wire anemometer (12) for determination of velocities. The wire was also used as a conventional four-lead resistance thermometer (13), and its dual use in both temperature and velocity measurements gave rise to the use of the term thermanemometer.

It should be emphasized that the thermanemometer as used was incapable of detecting the vectorial characteristics of velocity, and only the magnitude of this vector quantity, or speed, was indicated. Flow in the channel with no obstacle was probably unidirectional, but in the wake close to the cylinder velocities were not necessarily in the direction of bulk flow. Thus the term velocity will be used with the reservation that it designates only the magnitude of this vector quantity in certain regions of the wake. A pitot impact tube was used to calibrate the thermanemometer as a speed measuring device. The thermanemometer was used in most of the speed measurements in preference to the pitot tube due to the rapidity

with which measurements could be made and the fact that the dimensions of the wire allowed measurements close to obstacles to be made.

The circuit employed in connection with the thermanemometer is shown in Figure 6. This circuit permitted the use of the 0.5-mil platinum wire either as a device for measuring temperature or speed. For speed measurements switch S''' was closed in the down position and for temperature measurements in the up position (Figure 6). The circuit was designed for the measurement of speeds either by the constant resistance or constant current method of anemometry (12). In the present work the constant resistance method of operation was used exclusively in speed measurements, and in the application of this method switches S, S', and S''' were closed (Figure 6). The thermanemometer, T, in series with the 0.05 and 0.50 ohm resistors comprised one leg of a Wheatstone bridge whose balance was indicated by galvanometer G. The adjustment of settings on resistors D, P, and R determined the constant operating resistance (and therefore temperature) assumed by the wire when current flowed through the balanced bridge circuit. The amount of current flowing through the wire necessary to maintain this operating resistance was a function of the speed at the point where the wire was located. For a given air speed, resistors D', P', P'', and R' were adjusted until the bridge was balanced as indicated by galvanometer G.

A type K-2 potentiometer and a White double potentiometer were available for potentiometric measurements. A recently calibrated Type K-2 potentiometer was employed to measure the potential across the steel cylinder or across the heater element of the brass cylinder.

This potentiometer was also used to measure the current flowing through the steel cylinder or the heater element of the brass cylinder. From these potential and current measurements the rate of heat dissipation from the steel or brass cylinder and the average resistance and hence temperature of the steel cylinder were determined. The K-2 potentiometer was also used to determine the current flowing through and the potential across the thermanemometer. The surface temperatures on the brass cylinder indicated by the copper constantan thermocouples were read by means of a White double potentiometer.

A Mueller type bridge was used in the measurement of point temperatures when the thermanemometer was used as a conventional four-lead resistance thermometer. This bridge was also utilized in measurement of the bulk temperature of the air stream entering the conduit and the temperature of the oil flowing outside the upper and lower copper walls of the channel.

#### Experimental Methods and Sources of Error

The bulk temperature of the air entering the channel and the temperature of the oil circulating outside the upper and lower walls of the channel were maintained within  $0.02^{\circ}\text{F}$  of a predetermined value. A steady rate of thermal energy dissipation with an uncertainty of  $\pm 0.3$  per cent was maintained in the cylinder. The average temperature of the steel tube was established with an uncertainty of approximately  $\pm 0.5^{\circ}\text{F}$ . The temperatures indicated by the thermocouples imbedded in the brass tube were known with a precision of  $\pm 0.1^{\circ}\text{F}$ . However, it is uncertain whether or not the actual surface temperatures on the tube were indicated by the thermocouples.



Traverses were made at a suitable number of different longitudinal positions downstream of the cylinder, and at each position the temperature and air speed were determined at approximately twenty different elevations between the upper and lower walls. Check measurements were made in the wake at several longitudinal positions, and the data were found to be reproducible.

In the application of the thermomanometer to the measurement of air speed the wire was maintained at a constant resistance representing a temperature of approximately 200°F. The current required to bring the wire to a predetermined temperature is a function of the air speed, the temperature of the air flowing past the wire, and the temperature of the wire as expressed by King's equation for forced convection from a small heated wire in a steadily flowing air stream (12,14):

$$i^2 R_{hw} = (a + b\sqrt{\rho U})(R_{hw} - R_a) \quad (4)$$

a and b are constants which are a function of the physical properties of the air and the wire.

The thermomanometer was calibrated under isothermal conditions as a speed measuring device by means of a pitot tube (Figure 5) of conventional design (9). The value of the current, i, required to maintain the selected value of the constant hot wire resistance,  $R_{hw}$ , was measured for several velocities indicated by the pitot tube, and an essentially linear calibration curve resulted when  $\frac{i^2}{R_{hw} - R_a}$  was

plotted vs  $\sqrt{u}$  (Figure 7) as is predicted from King's equation.

There was a tendency for the calibration curve to shift with time; so the thermanemometer was calibrated at frequent time intervals. With increasing time the wire required less current to maintain it at the operating temperature for a constant speed. This behavior was consistent with the assumption that the heat transfer coefficient for forced convection from the wire decreased with time, and a plausible mechanism for this phenomenon was the accumulation of foreign material on the wire from the air. This mechanism was verified by the fact that the calibration curve was restored to its original position when the wire was raised to a temperature high enough to burn combustible foreign material off the wire.

The simple hot wire anemometer has inherent features which limit its ability to measure accurately the velocity at a point. As has been already mentioned one feature of the hot wire is that it is incapable of indicating the direction of velocity so that only the magnitude of this vector quantity can be measured. Near the cylinder well known Karman vortex trails are encountered in the wake (4,9,15,16,17), and in this region the velocities may be fluctuating both in magnitude and direction. Thus the hot wire measurements in the wake near the cylinder yield no information as to the direction of flow, and these data are therefore not amenable to an analysis such as a mass balance where a knowledge of both the magnitude and direction of velocity is required. Further downstream in the wake, however, it is probable that the direction of the point velocity is the same as that of the bulk air velocity, and thus both

the magnitude and direction of the air speed in this region are assumed to be known. The previous discussion assumes that the hot wire is able to respond to fluctuations in air speed without lag and to indicate the true mean air speed irrespective of the amplitude of the air speed fluctuations. The validity of these assumptions for actual operating conditions will be discussed.

The fact that fluctuating velocities are encountered both in the vortex trails behind a cylinder and in uniformly turbulent streams restricts the accuracy of the measurement of instantaneous air speeds with a hot wire anemometer under certain conditions. There is an upper limit to the frequency of velocity fluctuations to which a given hot wire can respond without lag. The ratio of the measured instantaneous speed to the actual speed is  $\frac{1}{\sqrt{1+K_4^2\omega^2}} K_4$  depends on the dimensions, physical properties, and operating conditions of the wire (4). The wire will lag behind the impressed instantaneous air speed by an angle whose tangent is  $K_4\omega$ .

Even if the wire responds to varying air speeds without appreciable lag, fluctuations of large amplitude cause error in the measured average speed. The instantaneous resistance of the wire,  $R_{hw}$ , will be related to the instantaneous speed in accordance with Equation (4). Since  $R_{hw}$  is small compared to the 0.55 ohm resistance in series with it in the leg of the Wheatstone bridge, the current through the wire is essentially constant and unaffected by the fluctuations in  $R_{hw}$  (Figure 6). A galvanometer with a high moment of inertia was used in the circuit so that an effective linear average,  $\bar{R}_{hw}$ , of the resistance fluctuations was measured when the galvanometer indicated a balance. The current needed to maintain

the wire at  $\bar{R}_{hw}$  is a measure of the time average value of the square root of the instantaneous speed as indicated by a modification of Equation (4):

$$l^2 \bar{R}_{hw} = (a + b\sqrt{\rho U})(\bar{R}_{hw} - \bar{R}_a) \quad (5)$$

A difference between the time average of the square root of the speeds and the desired time average of the instantaneous speeds is involved, and thus the speed indicated by the instrument is not the same as if the flow had been steady at the true average speed. The error involved increases with the amplitude of the fluctuation as is shown in Figure 8 for sinusoidal velocity fluctuations.

The probable accuracy of the thermomanometer used in the measurement of air speed in the wake of the cylinder will now be determined. Since no equipment was available for measuring the frequency or amplitude of fluctuating air speeds, experimental data taken under comparable conditions by other investigators are used in the ensuing analysis. Of primary concern is whether or not the wire responded without lag to the frequency of fluctuations encountered in the wake, and pertinent in this respect is the magnitude of the value of  $K_4 \omega$ . It appears that the fluctuations in the Karman vortex trails were approximately sinusoidal with a maximum frequency of 90 cycles per second (15,16,17). With the 0.5-mil wire used under the most adverse operating conditions of these experiments the maximum value of  $K_4$  was 0.002 seconds. The corresponding measured speed was 0.66 times the true speed for a frequency of 90 cycles

per second. Thus the effect of velocity fluctuations led to appreciable error in the measurement of air speeds in the relatively restricted zones near the cylinder where vortex trails were encountered (4). For average frequencies found in normal turbulence the error in the speed measurements was negligible. Thus the wire measured the air speed accurately in most portions of the wake.

The error in speed measurements due to large amplitudes of speed fluctuations is significant only in the vortex trails, where the ratio of the maximum amplitude of the fluctuating speed to the mean speed reaches a peak value of 0.44 at a distance of 0.1 inch downstream from the centerline of the cylinder (Figure 9). For sinusoidal fluctuations this ratio represents a value of the ratio of the measured average speed to the true average speed of 0.975 (Figure 8). For normal turbulence where amplitudes are small, the error is negligible.

When used as a conventional four-lead resistance thermometer, the thermomanometer was calibrated at a series of known temperatures in stagnant air in the channel. The influence of air speed on the measurement of the free stream temperature was taken into account by the use of an impact temperature correction (18), for bulk air velocities in excess of 40 feet per second. At 60 feet per second this correction amounted to  $-0.04^{\circ}\text{F}$ , which was applied to the apparent temperatures. This correction was established by an actual measurement of the apparent temperature indicated by the thermomanometer as a function of air speed for isothermal flow. Where lag in response was negligible, the wire followed the temperature fluctuations, and

the temperature indicated by the wire represented the desired time average value.

### Experimental Results

The results of the investigation of the temperature and velocity distribution in the wake of a heated cylinder for bulk velocities of 6.99, 12.7, 24.8, and 44.7 feet per second are presented in Table I, Parts 1 to 8 and in Figures 10 to 36. In most cases the walls of the conduit and the entering air were maintained at 100°F, and the rate of heat dissipation from the cylinder was kept at approximately 5.42 watts per inch length of the cylinder. Two traverses at a bulk velocity of 24.8 feet per second were made for a rate of heat transfer of 1.70 and 3.20 watts per inch for the above temperature conditions. One traverse at 24.8 feet per second was made for a rate of heat dissipation of 5.42 watts per inch, and the temperature of the upper wall was maintained at 130°F, the lower wall at 70°F, and the entering air at 100°F. For each of the four bulk air velocities the temperature and air speed distribution are presented in two different fashions. In the first case the fraction of the distance between the walls is plotted versus the temperature or air speed, and each curve represents a traverse in the wake at a particular position downstream from the cylinder (Figures 10 and 28).

In the second case the data just described are cross plotted and presented as fields of temperature or air speed in the wake.

Fraction of distance between the walls is plotted versus distance downstream from the cylinder, and lines of constant temperature and velocity respectively are shown (Figures 11 and 29).

For a bulk velocity of 6.99 feet per second the temperature data are shown in Figures 10 and 11 and are tabulated in Table I, Part 1. The temperature of the walls and entering air is 100°F. The Reynolds number based on the channel is 4,220 and 562 based on the cylinder diameter. The average temperature of the cylinder for a rate of heat dissipation of 5.42 watts per inch is 368.2°F. It is noteworthy that for traverses near the cylinder relatively complex temperature profiles occur. Some of the details of the traverse at 0.15 inch downstream from the centerline of the cylinder (Figure 10) will be analyzed. The temperature of the air remains at 100°F from the upper wall to the region opposite the upper edge of the cylinder, where a sudden rise of temperature occurs. A temperature of 250.8°F is attained at an ordinate of about 0.65. The upper and lower edges of the cylinder are represented by ordinates of about 0.63 and 0.37 respectively. Close to the cylinder, the Karman vortex trails are known to exist in the zones near the upper and lower edges of the cylinder. After reaching a high value opposite the upper edge of the cylinder, the temperature decreases to about 216°F and then rises to 260°F at the center of the wake. In Figure 28 the corresponding speed traverse close to the cylinder is shown. It is evident that the

rise in temperature at the center of the wake (Figure 10) occurs in the region where the speed is low (Figure 28).

The temperature distribution is relatively symmetrical about the 0.5 ordinate except for the fact that the value of the high temperature attained opposite the lower edge of the cylinder is below the value of the high temperature reached opposite the upper edge (Figure 10). One possible explanation of this effect is that natural convection causes the upper part of the wake to attain a higher temperature than the lower part. The phenomenon is more prominent at low bulk velocities where the surface temperature of the cylinder is high, and forced convection does not obscure the effect of natural convection. Further downstream in the wake the temperature distribution becomes less complex. At 1.29 inches downstream from the centerline of the cylinder the temperature distribution is relatively simple, and it is assumed that the eddies causing the complexity of the profiles near the cylinder have been dissipated. The velocity profile is also relatively simple at 1.29 inches downstream (Figure 28).

It is noteworthy that the width of the wake,  $y_b'$ , increases with distance downstream (Figure 10). The edge of the wake is defined as that point in the wake where the undisturbed stream temperature is reestablished. The width of the wake is found to be directly proportional to  $x^{\frac{1}{2}}$  as will be discussed in more detail subsequently. Due to the relatively large diameter of the cylinder, 0.190 inch, compared to the distance between the walls, 0.75 inch, the edge of the wake approaches the walls at a relatively short distance downstream of the cylinder ( $x=1.29$  inches in Figure 10). At 9.43 inches



downstream the temperature at the center of the wake is  $107.3^{\circ}\text{F}$ , and the temperature at the center of the wake in general is found to vary directly with  $x^{-\frac{1}{2}}$ .

In Figure 11 the temperature field is graphically portrayed, and very high vertical and horizontal temperature gradients in the vicinity of the cylinder are in evidence. The cylinder is drawn to scale, and the magnitude of the width of the channel and the wake are shown in relation to the diameter of the cylinder.

For a bulk velocity of 12.7 feet per second the temperature distribution is shown in Figures 12 and 13 and is tabulated in Table I, Part 2. The walls of the channel and the air are at  $100^{\circ}\text{F}$ . The Reynolds number based on the channel is 7,630 and based on the cylinder diameter is 1,221. The average temperature of the cylinder for a rate of heat dissipation of 5.41 watts per inch is  $310.8^{\circ}\text{F}$ . Again is evident the asymmetry of the upper and lower maximum points in the temperature profiles, attributed to natural convection. At a distance of 0.19 inch downstream from the centerline of the cylinder and opposite the upper edge, a temperature of  $179.7^{\circ}\text{F}$  is attained (Figure 12). The corresponding temperature in the lower part of the wake is  $176.3^{\circ}\text{F}$ ,  $3.4^{\circ}\text{F}$  less than in the upper part of the wake. The increase in the width of the wake with distance downstream is again evident in Figure 12.

The temperature field is portrayed in Figure 13. In Figure 14 is presented a photograph of air flowing past a heated cylinder (19). Because of the change of refractive index with temperature, the hot air appears brighter than the cooler air, and pictorial evidence of

an isothermal region in the wake is obtained. There is a marked similarity between the shape of the  $147^{\circ}\text{F}$  isotherm in Figure 13 and the outline of the isothermal region in Figure 14.

For a bulk velocity of 24.8 feet per second, the temperature distribution is included for three rates of dissipation of heat: 1.70, 3.20, and 5.43 watts per inch in Figures 15 to 18 and Table I, Parts 3 to 5. The walls of the conduit and the air are at  $100^{\circ}\text{F}$ . The Reynolds number based on the channel is 15,200 and on the cylinder diameter approximately 2,285 for the three cases. The average temperatures of the cylinder are  $152.1$ ,  $198.3$ , and  $265.8^{\circ}\text{F}$  respectively. Common to all temperature traverses is the fact that the curves for various distances downstream intersect at a common point in the upper and lower portions of the wake (at about  $103^{\circ}\text{F}$  in Figure 17). In Figure 18 this phenomenon is illustrated by the fact that both  $103^{\circ}\text{F}$  isotherms are horizontal for a relatively large distance downstream.

By a comparison of Figures 15, 16, and 17 it is obvious that the spatial extent of the complex temperature profiles diminishes with decreasing rates of heat dissipation. The width of the wake however remains constant in spite of variation in the rate of heat dissipation. In Figure 17 the maximum air temperature at a distance of 0.15 inch downstream from the centerline of the cylinder is  $147.2^{\circ}\text{F}$  in the upper portion of the wake and  $146.6^{\circ}\text{F}$  in the lower portion. Thus the profiles near the cylinder become more symmetrical with increasing bulk velocities as is seen in Figures 10, 12, and 17 for 5.43 watts per inch. Figure 18 portrays the temperature field for 5.43 watts per inches at 24.8 feet per second.

For a bulk velocity of 24.8 feet per second with the upper wall at 130°F, the lower wall at 70°F, and the entering air at 100°F, the temperature distribution is shown in Figure 19 and Table I, Part 6. The average surface temperature of the cylinder is 285.2°F at a rate of heat dissipation of 5.42 watts per inch. The undisturbed stream temperature profile is similar to the S-shaped curve for a distance of 9.43 inches downstream (Figure 19). It is interesting to note that by superposing the profile at 9.43 inches (Figure 19) on the profiles at various distances downstream in Figure 17, that the profiles of Figure 19 are approximately reproduced.

At a bulk velocity of 44.7 feet per second the temperature distribution is shown in Figures 20 and 21 and Table I, Part 7. The walls of the channel and the entering air are at 100°F. The Reynolds number based on the channel is 26,900 and on the cylinder diameter is 4,400. The average surface temperature of the cylinder is 206.2°F. The effect of natural convection at a distance downstream of 0.13 inch (Figure 20) is obscured within the precision of the measurements. Figure 21 gives the temperature field at this velocity.

A review of the temperature distribution data presented in Figures 10,12,15,16,17, and 20 indicates that the region of complex temperature profiles in the wake decreases in spatial extent as the bulk velocity is increased or the rate of heat dissipation decreases. However, the width of the wake at a particular distance downstream from the cylinder is independent of the bulk velocity or rate of heat dissipation. In Figures 11,13,18, and 21 at a distance of 0.5 inch downstream from the centerline of the cylinder the average temperature

in the wake decreases with increasing bulk velocities for a constant rate of heat dissipation. This phenomenon is obvious from the fact that the change in the bulk temperature of the air is approximately inversely proportional to the mass of air flowing past the heated cylinder in unit time, for a constant rate of heat dissipation.

In Figure 22 is plotted the temperature at the center of the wake versus  $x^{-\frac{1}{2}}$  for four bulk velocities. A linear relationship exists between the functions for a given bulk velocity. In Figure 23 is shown the linear relationship on a logarithmic plot between the width of the wake,  $y'_b$ , and the distance downstream,  $x$ . The points shown represent data for four bulk velocities, and it is seen that the slope of the line is not a function of bulk velocity. From the slope of the line, it develops that  $y'_b$  is a linear function of  $x^{\frac{1}{2}}$ . This relationship is compatible with dimensional analysis as will be discussed subsequently.

The variation in the surface temperature of the brass cylinder around its circumference was measured with thermocouples, and the results are presented for various values of power dissipation at bulk velocities of 14.4 and 23.8 feet per second in Figures 24 and 25 respectively and Table II. In these figures polar coordinates are utilized to show the circumferential temperature distribution. The polar angles designate the position on the circumference of the cylinder relative to the direction of the flowing stream, and the radial distances denote the magnitude of the temperature at a given position on the surface of the cylinder. As would be expected the average surface temperature of the cylinder at a constant rate

of energy dissipation is higher the lower the velocity. In Figure 24 each curve demonstrates the fact that the leading edge of the cylinder apparently is at a lower temperature than the trailing edge. This phenomenon could be explained by the fact that the air speed is low directly behind the cylinder (Figure 30), but because of the uncertainty in localizing the measured temperatures, conclusions drawn from the present data are made with reservation. The general shape of these curves conforms with curves presented in the literature (20).

In Figure 26 and Table III are presented experimental values of the average surface temperature of the steel heated cylinder as a function of the rate of heat dissipation for four bulk velocities. For each bulk velocity it is seen that the rate of heat dissipation increases linearly with the surface temperature of the cylinder. This dependence would be expected from King's relationship for forced convection from small heated cylinders (Equation 3) (14). Thus  $h$ , the overall heat transfer coefficient, is essentially independent of the average surface temperature of the cylinder for a given Reynolds number. The heat transfer rate increases in a regular fashion with Reynolds number for a given surface temperature. The implication of these relationships is that the values of the heat transfer coefficient and of the eddy quantities are dependent on Reynolds number, which is more affected by changes in the bulk velocity of flow than by changes in the surface temperature of the cylinder.

The data of Figure 26 are plotted in the conventional form of dimensionless parameters in Figure 27. Nusselt number,  $hD_o/k_f$ , is

plotted versus Reynolds number,  $D_o U \rho / \mu_f$ . A set of three points from each curve of Figure 26 is included in Figure 27. These points represent average film temperatures of 125, 150, and 175°F, the highest film temperature corresponding to the lowest value of Nusselt number. The curve is based on data in the literature for the heating of gases flowing normal to a single cylinder by forced convection (20). It is seen that the data of the present investigation are in agreement with those of the other sources.

The air speed distribution for a bulk velocity of 6.99 feet per second is shown in Figure 28 and Table I, Part 1. At a distance of 0.23 inch from the centerline of the cylinder in Figure 28 the speed reaches a maximum of 12.3 feet per second at the top of the cylinder, suddenly decreases to a minimum of 0.2 feet per second and rises to a value of 0.5 feet per second at the center of the wake. The very large speed gradient opposite the upper and lower edges of the cylinder and the rise in speed at the center of the wake near the cylinder occur where the Karman vortex system is known to prevail (4,9).

The maximum speed of 12.3 feet per second, 5.3 feet per second above the bulk velocity, demonstrates the fact that the free cross-section area of the conduit has been reduced materially due to the presence of the cylinder, and thus speed as well as temperature measurements in the wake may be affected by the walls of the channel. At a further distance downstream the maximum speeds attained are less than in the regions close to the cylinder, and there is no rise in air speed at the center of the wake. At 9.43 inches downstream the approximate normal velocity profile of the empty channel has been

attained. In Figure 29 the air speed field is shown by constant speed lines. The rise in speed at the center of the wake and the large air speed gradient opposite the upper and lower edges of the cylinder are evident at 0.3 inch downstream.

The air speed distribution for bulk velocities of 12.7, 24.8, and 44.7 feet per second are similarly represented in Figures 30, 32, and 34, Table I, Parts 2, 5, and 7. The corresponding air speed fields are shown in Figures 29, 31, and 33, and the rise in air speed near the center of the wake and the large air speed gradient opposite the upper and lower edges of the cylinder are evident around 0.2 to 0.3 inch downstream. The region close to the cylinder (Figures 28, 30, 32, and 34) corresponds to the zone of complex temperature distribution (Figures 10, 12, 15, 16, 17, and 20). As was the case with temperature, the region of complex speed distribution decreases in spatial extent as the bulk velocity increases. These complex regions are associated with the Karman vortex system, and therefore the rapidity with which the system is dissipated is seen to increase with bulk velocity. The general shape of these complex air speed curves is verified by data from other sources (4) (Figure 9). The speed measurements shown in Figure 9 were made with electronic circuits which compensated for the lag in response of the wire to the high frequency fluctuations encountered near the cylinder.

It was found that the speed distribution for a given bulk velocity was relatively independent of the temperature field. For each of the four bulk velocities the air speed distribution was investigated with the cylinder unheated. The air speed distribution was found to be independent of the temperature field for the range of conditions

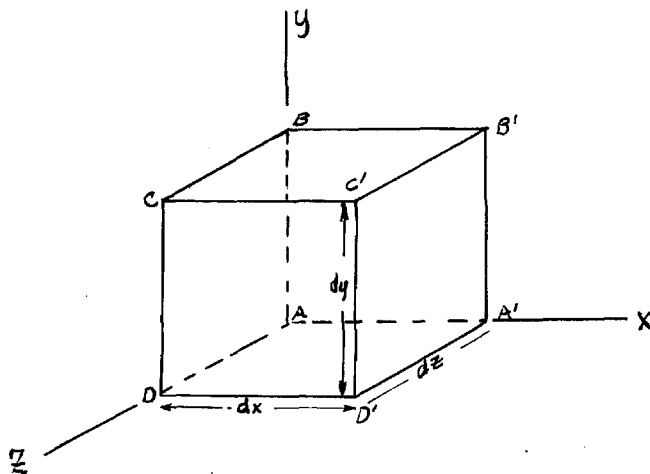
investigated as is shown by a comparison of Figures 34 and 36.

It is noteworthy that the temperature field in the zone near the cylinder and at the center of the wake (Figures 11, 13, 18, and 21) is very similar to the corresponding speed field in the same region (Figures 29, 31, 33, and 35 respectively).

### Theoretical Analysis of Results

A knowledge of the values of eddy conductivity and viscosity provides the engineer with a useful means of predicting the temperature and velocity distributions in a flowing fluid for a given set of physical conditions. Mathematical equations will be derived relating these eddy quantities to the pertinent functions of state and flow conditions. The equation for eddy conductivity will be derived from a consideration of the various possible forms of energy transferred to or from a volume element of the fluid. The equation for eddy viscosity will be derived from a consideration of forces in the  $x$ -direction on a volume element of the fluid.

In the derivation of an equation involving eddy conductivity, consider an infinitesimal volume element through which a fluid is flowing:





An energy balance will be set up by a consideration of all possible forms of energy entering or leaving the faces of the volume element. Steady state conditions will be assumed to prevail. An energy balance over all faces is given by (21):

$$\sum (dH + dh + d(\underline{K.E.}) + \underline{W} - q) = 0 \quad (6)$$

It will be assumed that potential energy, kinetic energy and work terms may be neglected in comparison to the other terms. Equation (6) then becomes:

$$\sum dH = \sum q \quad (7)$$

To what extent these assumptions are valid will be shown subsequently. Heat will be conducted into the lattice through the various faces in a time  $d\theta$  in accordance with Newton's law of conduction. The concept of superposing the turbulent agent,  $\epsilon_c$ , upon the thermometric conductivity,  $K$ , will be used.

Heat conducted into the lattice in the time  $d\theta$  in the x-direction through face ABCD is:

$$- \sigma C_p (\epsilon_{cx} + K) \frac{\partial t}{\partial x} d\theta dy dz \quad (8)$$

and out through face A'B'C'D' is:

$$\left\{ -\sigma C_p (\epsilon_{cx} + K) \frac{\partial t}{\partial x} + \frac{\partial}{\partial x} \left[ -\sigma C_p (\epsilon_{cx} + K) \frac{\partial t}{\partial x} \right] dx \right\} d\theta dy dz \quad (9)$$

A net transfer of heat in the x-direction from (8) and (9):

$$\dot{q}_x = \frac{\partial}{\partial x} \left[ \sigma C_p (\epsilon_{cx} + \kappa) \frac{\partial t}{\partial x} \right] d\theta dx dy dz \quad (10)$$

From a similar consideration of the remaining faces, it follows that the total heat transferred by conduction into the volume element is:

$$\sum \dot{q} = \left\{ \frac{\partial}{\partial x} \left[ \sigma C_p (\epsilon_{cx} + \kappa) \frac{\partial t}{\partial x} \right] + \frac{\partial}{\partial y} \left[ \sigma C_p (\epsilon_{cy} + \kappa) \frac{\partial t}{\partial y} \right] + \frac{\partial}{\partial z} \left[ \sigma C_p (\epsilon_{cz} + \kappa) \frac{\partial t}{\partial z} \right] \right\} d\theta dx dy dz \quad (11)$$

The enthalpy of material passing through the face ABCD in the x-direction in time  $d\theta$  is:

$$(\sigma u H) d\theta dy dz \quad (12)$$

and the enthalpy of material leaving the element through face A'B'C'D' is:

$$\left[ \sigma u H + \frac{\partial (\sigma u H)}{\partial x} dx \right] d\theta dy dz \quad (13)$$

The net change in enthalpy of the fluid between the faces is:

$$\sum dH_x = \frac{\partial}{\partial x}(\sigma u H) d\theta dx dy dz \quad (14)$$

The total change in enthalpy of the material passing through the element in time,  $d\theta$ , applying this analysis to all faces is:

$$\sum dH = \left\{ \frac{\partial}{\partial x}(\sigma u H) + \frac{\partial}{\partial y}(\sigma v H) + \frac{\partial}{\partial z}(\sigma s H) \right\} d\theta dx dy dz \quad (15)$$

From the hydrodynamical equation of continuity for steady state conditions (22,23):

$$\frac{\partial(u\sigma)}{\partial x} + \frac{\partial(v\sigma)}{\partial y} + \frac{\partial(s\sigma)}{\partial z} = 0 \quad (16)$$

Combining Equations (7), (15), and (16) there results:

$$\begin{aligned} \sigma \left[ u \frac{\partial H}{\partial x} + v \frac{\partial H}{\partial y} + s \frac{\partial H}{\partial z} \right] &= \frac{\partial}{\partial x} \left[ \sigma C_p (\epsilon_{cx} + K) \frac{\partial t}{\partial x} \right] \\ &+ \frac{\partial}{\partial y} \left[ \sigma C_p (\epsilon_{cy} + K) \frac{\partial t}{\partial y} \right] + \frac{\partial}{\partial z} \left[ \sigma C_p (\epsilon_{cz} + K) \frac{\partial t}{\partial z} \right] \end{aligned} \quad (17)$$

From the assumption that the working fluid is a perfect gas (21):

$$\frac{dH}{dT} = C_p \quad (18)$$

Combining Equations (17) and (18):

$$\begin{aligned} \sigma C_p \left[ u \frac{\partial t}{\partial x} + v \frac{\partial t}{\partial y} + s \frac{\partial t}{\partial z} \right] &= \frac{\partial}{\partial x} \left[ \sigma C_p (\epsilon_{cx} + K) \frac{\partial t}{\partial x} \right] \\ &+ \frac{\partial}{\partial y} \left[ \sigma C_p (\epsilon_{cy} + K) \frac{\partial t}{\partial y} \right] + \frac{\partial}{\partial z} \left[ \sigma C_p (\epsilon_{cz} + K) \frac{\partial t}{\partial z} \right] \end{aligned} \quad (19)$$

Without the simplifying assumptions which led to Equation (7), an equation of the same form as Equation (19) results except for a term for the work against viscous forces and a term  $\frac{DP}{D\theta}$  (9). The latter term is negligible under the condition of these experiments, and it is assumed that the first term may also be neglected. For two-dimensional flow,  $S=0$  and  $\frac{\partial t}{\partial z}=0$ . Assume that the region in the wake is far enough downstream of the cylinder so that  $V=0$ . Then Equation (19) becomes:

$$\sigma C_p u \frac{\partial t}{\partial x} = \frac{\partial}{\partial x} \left[ \sigma C_p (\epsilon_{cx} + K) \frac{\partial t}{\partial x} \right] + \frac{\partial}{\partial y} \left[ \sigma C_p (\epsilon_{cy} + K) \frac{\partial t}{\partial y} \right] \quad (20)$$

Thus because of the non-vectorial nature of energy, Equation (20) involves eddy quantities in the x and y-direction.

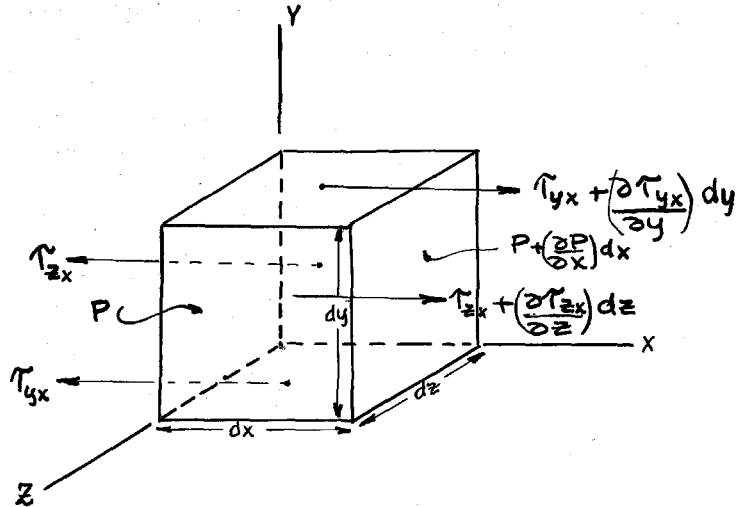
Multiplying Equation (20) by dy and integrating from  $y=y'=0$  to  $y=y'$ , since  $\frac{\partial t}{\partial y}=0$  at  $y'=0$ :

$$\epsilon_{cy} + K = \frac{\int_0^{y'} \sigma C_p u \frac{\partial t}{\partial x} dy - \int_0^{y'} \frac{\partial}{\partial x} [\sigma C_p (\epsilon_{cx} + K) \frac{\partial t}{\partial x}] dy}{\sigma C_p \frac{\partial t}{\partial y}} \quad (21)$$

Under the experimental conditions it was found that as an approximation the second term could be neglected, so that Equation (21) becomes:

$$\epsilon_{cy} + K = \frac{\int_0^{y'} \sigma C_p u \frac{\partial t}{\partial x} dy}{\sigma C_p \frac{\partial t}{\partial y}} \quad (22)$$

In the derivation of an equation for eddy viscosity consider an infinitesimal volume element of a viscous, compressible fluid:



Forces acting on the fluid in the x-direction will be considered.

Body forces such as due to gravity will be neglected, and only surface forces will be considered as shown above.

The resultant force in the x-direction is:

$$F_x = \left[ \left( \frac{\partial \tau_{yx}}{\partial y} \right) dy \right] dx dz + \left[ \left( \frac{\partial \tau_{zx}}{\partial z} \right) dz \right] dx dy - \left[ \left( \frac{\partial P}{\partial x} \right) dx \right] dy dz \quad (23)$$

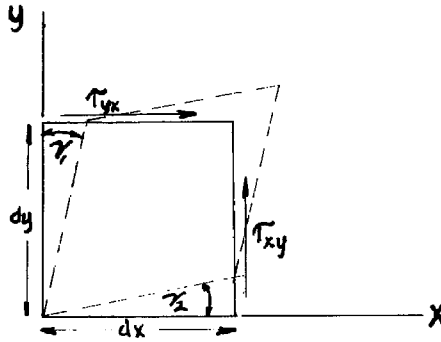
From Newton's law of motion (22): Force = mass x acceleration,

$$F_x = \rho dx dy dz \frac{Du}{Dt} \quad (24)$$

Equating Equations (23) and (24):

$$\rho \frac{Du}{Dt} = \left[ -\left(\frac{\partial P}{\partial x}\right) + \left(\frac{\partial \tau_{yx}}{\partial y}\right) + \left(\frac{\partial \tau_{zx}}{\partial z}\right) \right] \quad (25)$$

In order to relate the shear forces to the velocity gradient, consider an infinitesimal square:



The shear stresses  $\tau_{xy} = \tau_{yx}$  cause a rate of change in the original  $90^\circ$  angle (22):

$$\tau_{yx} = \rho (\epsilon_{my} + \nu) \left( \frac{\partial \gamma_1}{\partial \theta} + \frac{\partial \gamma_2}{\partial \theta} \right) \quad (26)$$

where the eddy viscosity,  $\epsilon_{my}$ , is superposed on the kinematic viscosity,  $\nu$ .

Since,  $\frac{\partial \gamma_1}{\partial \theta} = \frac{\partial}{\partial y} \frac{\partial x}{\partial \theta} = \frac{\partial u}{\partial y}$  and  $\frac{\partial \gamma_2}{\partial \theta} = \frac{\partial}{\partial x} \frac{\partial y}{\partial \theta} = \frac{\partial v}{\partial x}$ .

Equation (26) becomes:

$$\tau_{yx} = \rho (\epsilon_{my} + \gamma) \left( \frac{\partial u}{\partial y} + \frac{\partial v}{\partial x} \right) \quad (27)$$

By definition (22):

$$\frac{Du}{Dt} = \frac{\partial u}{\partial t} + u \frac{\partial u}{\partial x} + v \frac{\partial u}{\partial y} + s \frac{\partial u}{\partial z} \quad (28)$$

For the case of two-dimensional, steady flow as exists in the wake of the cylinder in these experiments

$s = 0$ ,  $\frac{\partial u}{\partial z} = 0$ , and  $\frac{\partial u}{\partial t} = 0$ . Equation (28) becomes:

$$\frac{Du}{Dt} = u \frac{\partial u}{\partial x} + v \frac{\partial u}{\partial y} \quad (29)$$

and Equation (25) becomes:

$$\rho \left( u \frac{\partial u}{\partial x} + v \frac{\partial u}{\partial y} \right) = \left[ - \left( \frac{\partial P}{\partial x} \right) + \left( \frac{\partial \tau_{yx}}{\partial y} \right) + \left( \frac{\partial \tau_{zx}}{\partial z} \right) \right] \quad (30)$$

Since  $\frac{\partial u}{\partial z} = 0$ ,  $\tau_{zx}$  and therefore  $\left( \frac{\partial \tau_{zx}}{\partial z} \right) = 0$ . Thus

Equation (30) becomes:

$$\rho \left( u \frac{\partial u}{\partial x} + v \frac{\partial u}{\partial y} \right) = - \left( \frac{\partial P}{\partial x} \right) + \frac{\partial \tau_{yx}}{\partial y} \quad (31)$$



Integrating Equation (31) from  $y=y'=0$  to  $y=y'$ , since  $\tau_{yx}=0$  at  $y'=0$

$$\tau_{yx} = \int_0^{y'} \rho \left( u \frac{\partial u}{\partial x} + v \frac{\partial u}{\partial y} \right) dy + \int_0^{y'} \frac{\partial P}{\partial x} dy \quad (32)$$

Substituting Equation (27) in Equation (32) and solving for  $(\epsilon_{my} + \nu)$ :

$$\epsilon_{my} + \nu = \frac{\int_0^{y'} \rho \left( u \frac{\partial u}{\partial x} + v \frac{\partial u}{\partial y} \right) dy + \int_0^{y'} \frac{\partial P}{\partial x} dy}{\rho \left( \frac{\partial u}{\partial y} + \frac{\partial v}{\partial x} \right)} \quad (33)$$

Assume that the position in the wake is far enough downstream so that  $v=0$ ; then Equation (33) becomes:

$$\epsilon_{my} + \nu = \frac{\int_0^{y'} \rho \left( u \frac{\partial u}{\partial x} \right) dy + \int_0^{y'} \frac{\partial P}{\partial x} dy}{\rho \frac{\partial u}{\partial y}} \quad (34)$$

In Figure 37 and Table IV are shown values of eddy conductivity and eddy viscosity for a bulk velocity of 6.99 and 24.8 feet per second. At 6.99 feet per second the data are given for a distance of 0.72 inch downstream, and at 24.8 feet per second for a distance of 0.58 inch downstream. It is seen that the values of the eddy quantities increase with bulk velocity as would be expected (Figure 37). The shape of the eddy viscosity curves is seen to be complex. The ratio of the eddy quantities varies appreciably from unity except at an ordinate of around 0.60 (Figure 37 and Table IV).

Theories of the dynamics of turbulent flow yield relationships which like eddy quantities are of value to the chemical engineer in the prediction of temperature and velocity distributions existing in flowing fluids for various physical conditions. Two such theories of the mechanism of turbulence are Prandtl's momentum transfer theory and Taylor's vorticity transfer theory (24). A comprehensive analysis of these theories is presented in the literature (9,24,25,26), so that only a brief discussion of the details of the equations based on the theories will be included here.

The equation of motion representing Prandtl's theory of momentum transfer applied to the two-dimensional wake of a heated obstacle far downstream of the obstacle, is:

$$u_b \frac{\partial u}{\partial x} = \frac{\partial}{\partial y} \left( \epsilon \frac{\partial u}{\partial y} \right) \quad (35)$$

Specifically,  $\epsilon$ , is the eddy viscosity term, but in the subsequent analysis Reynolds analogy (3,20) is assumed to be valid, and thus  $\epsilon_m = \epsilon_c = \epsilon$ .

The corresponding equation of motion according to Taylor's vorticity transfer theory applied to the two-dimensional wake of a heated obstacle far downstream of the obstacle, is:

$$u_b \frac{\partial u}{\partial x} = \epsilon \frac{\partial^2 u}{\partial y^2} \quad (36)$$

Prandtl defines  $\epsilon$  as:

$$\epsilon = l^2 \frac{\partial u}{\partial y'} \quad (37)$$

where  $l$  is the mixing length assumed not to be a function of  $y'$ . Substituting Equation (37) in Equations (35) and (36),

$$u_b \frac{\partial u}{\partial x} = 2l^2 \frac{\partial u}{\partial y'} \frac{\partial^2 u}{\partial y'^2} \quad \text{Momentum transfer theory} \quad (38)$$

$$u_b \frac{\partial u}{\partial x} = l^2 \frac{\partial u}{\partial y'} \frac{\partial^2 u}{\partial y'^2} \quad \text{Vorticity transfer theory} \quad (39)$$

From dimensional analysis (9) the width of the wake is found to be proportional to the square root of the distance downstream from the obstacle. This result was found experimentally in the present set of measurements (Figure 23).

$$y'_b = K_5 x^{1/2} \quad (40)$$

Prandtl assumes that at a sufficient distance downstream of the obstacle, the mixing length is proportional to the width of the wake:

$$1 = K_6 y_b' \quad (41)$$

Combining Equations (40) and (41)

$$1^2 = K_7 x \quad (42)$$

Substituting Equation (42) in Equations (38) and (39):

$$u_b \frac{\partial u}{\partial x} = 2 K_7 x \frac{\partial u}{\partial y'} \frac{\partial^2 u}{\partial y'^2} \quad \text{Momentum transfer theory} \quad (43)$$

$$u_b \frac{\partial u}{\partial x} = K_7 x \frac{\partial u}{\partial y'} \frac{\partial^2 u}{\partial y'^2} \quad \text{Vorticity transfer theory} \quad (44)$$

Solving these differential Equations (43) and (44) and expressing the results in a convenient form:

$$\frac{u_b - u}{u_b - u_c} = \left[ 1 - \left( \frac{y'}{y_b'} \right)^{3/2} \right]^2 \quad \text{for both theories} \quad (45)$$

Thus the velocity distribution predicted is the same for both theories.

A criterion for verifying either of the two theories lies in an analysis of the temperature distribution data in the wake of a heated obstacle.

Neglecting the term  $\epsilon_{cx} + \kappa$  in Equation (20), assuming that far downstream  $U_b = U$  and that  $\sigma C_p$  is constant in the x-direction, and assuming Reynolds analogy valid:

$$U_b \frac{\partial t}{\partial x} = \frac{\partial}{\partial y} \left( \epsilon \frac{\partial t}{\partial y} \right) \quad (46)$$

which is not based on either theory. From a comparison of Equation (35) for the momentum transfer theory and Equation (46) it is evident from a qualitative point of view that the temperature and velocity distributions should be of the same form, and this fact is verified by mathematical analysis. Thus by Prandtl's momentum transfer theory:

$$\frac{t - t_o}{t_c - t_o} = \left[ 1 - \left( \frac{y'}{y_b'} \right)^{3/2} \right]^2 \quad \text{Momentum transfer theory} \quad (47)$$

By manipulating Equation (36) for the vorticity transfer theory and Equation (46), an expression for the temperature distribution on the basis of Taylor's vorticity transfer theory results:

$$\frac{t - t_o}{t_c - t_o} = \left[ 1 - \left( \frac{y'}{y_b'} \right)^{3/2} \right] \quad \text{Vorticity transfer theory} \quad (48)$$

Thus the two theories predict different temperature distributions in the wake, and a test of the validity of each theory is obtained

by the use of empirical temperature distribution data. The results of the test of the data are shown in Figures 38-42, and Table V.

In Figure 38 the upper curve is based on Taylor's vorticity transfer theory, Equation (48); whereas the lower curve is based on Prandtl's momentum transfer theory, Equation (47). The experimental points for a distance of 0.72 inch and 1.29 inches downstream for a bulk velocity of 6.99 feet per second are shown in Figure 38 and Table V. It is evident that the empirical data conform well to Prandtl's momentum transfer theory. In Figure 39 for a bulk velocity of 12.7 feet per second again Prandtl's theory is verified. Similarly for bulk velocities of 24.8 and 44.7 feet per second in Figures 40 and 41, Prandtl's theory is substantiated by the experimental data. All of the experimental points were chosen at distances sufficiently far downstream from the cylinder so that the complex region of the wake near the cylinder, where Equations (47) and (48) are not valid, was avoided (Figures 10, 12, 17, and 20).

In Figure 42 for a bulk velocity of 44.7 feet per second, both the temperature ratio,  $\frac{t - t_c}{t_c - t_o}$ , and the velocity ratio,  $\frac{u_b - u}{u_b - u_c}$ , are plotted versus  $y'/y'_b$ . Because of the uncertainty in defining the width of the wake from the speed distribution data (Figure 28), the width of the wake,  $y'_b$ , was determined from the temperature distribution data (Figure 23). For a distance of 0.40 inch downstream the temperature and velocity data are seen to deviate

slightly from the simplified theoretical equation based on Prandtl's theory Equations (45) and (47) respectively. Close to the cylinder the temperature and velocity data deviate from the theoretical curves based on simplifying assumptions, but it is noteworthy that in each case the shapes of the empirical temperature and velocity curves are similar. The resemblance in the shapes of the curves is in keeping with the fact that Equation (35) based on Prandtl's momentum transfer theory is of the same form as Equation (46). The similarity in the curves is also qualitatively a verification of the Reynolds analogy since it implies the equality of eddy conductivity and eddy viscosity in Equations (46) and (35) respectively.

#### Conclusions

The temperature and velocity field in the wake of a heated cylinder has been explored over a range of bulk velocities of from 6.99 to 44.7 feet per second and at several rates of heat dissipation. These temperature and velocity distribution data have been used to evaluate numerical values of eddy viscosity and eddy conductivity and to test theories of turbulence. Measurements of rates of heat dissipation from the cylinder as a function of bulk velocity have been used to obtain correlations between dimensionless parameters. Surface temperatures on the cylinder have been obtained as functions of a position on the circumference.

As a logical sequence to the data obtained in this investigation the following research program is suggested. In order to minimize the effect that the walls of the conduit have on the velocity profiles in the wake of a cylinder a tube of smaller outside diameter than the one used in these experiments is recommended.

The use of a cylinder as small as 0.020 inch in outside diameter would be advisable. Emphasis should be placed on a thorough investigation of the temperature and velocity distribution in parts of the wake far enough downstream so that complex distributions are not encountered. The data should be complete enough so that derivatives in the x and y-direction can be precisely determined for the calculation of eddy quantities.

Measurements of the eddy quantities as a function of the intensity of turbulence would be of value. The intensity of turbulence (27) is automatically fixed in uniformly flowing turbulent streams in the unobstructed channel. However, the intensity of turbulence in the wake of a heated cylinder can be varied by placing screens upstream of the cylinder. The size of the screen mesh can be used to vary the intensity of turbulence. A means for measuring the intensity of turbulence must be provided. The simple diffusion method of measuring the intensity of turbulence from the temperature distribution in the wake of the cylinder may be used (28). If a method independent of temperature distribution measurements is desired, a suitable hot wire assembly can be used to measure fluctuating components of velocity and therefore intensity of turbulence (27,29).

Not only the eddy quantities but the overall heat transfer coefficient from the cylinder can be determined as a function of the intensity of turbulence (7).



## Nomenclature

### English letters

a	Dimensional constant for thermanemometer calibration equation
b	Dimensional constant for thermanemometer calibration equation
c	Concentration, $\text{lbs/ft}^3$
$c_p$	Isobaric heat capacity, $\text{B.t.u./lb } ^\circ\text{F}$
D	Molecular diffusivity, $\text{ft}^2/\text{sec}$
$D_o$	Outside diameter of cylinder, ft or in
F	Force, lb
g	Acceleration due to gravity, $\text{ft/sec}^2$
h	Heat transfer coefficient, $\text{B.t.u./sec ft}^2 ^\circ\text{F}$
$\underline{h}$	Elevation above datum plane, ft-lb
H	Specific enthalpy, $\text{B.t.u./lb}$
$\underline{H}$	Total enthalpy, $\text{B.t.u.}$
i	Current, amperes
k	Thermal conductivity, $\text{B.t.u. ft/sec ft}^2 ^\circ\text{F}$
$k_f$	Thermal conductivity at arithmetic mean of wall and fluid temperature, $\text{B.t.u. ft/sec ft}^2 ^\circ\text{F}$
$\underline{K.E.}$	Total kinetic energy, ft-lb
K	Constant
l	Mixing length, ft
M	Rate of transfer of material, $\text{lb/ft}^2 \text{ sec}$
P	Pressure, $\text{lb/ft}^2$
$\underline{q}$	Total heat, $\text{B.t.u.}$
$\dot{Q}$	Rate of heat transfer per unit area, $\text{B.t.u./sec ft}^2$

$R$	Resistance, ohms
$R_a$	Resistance of thermanemometer at air temperature, ohms
$R_{hw}$	Resistance of thermanemometer at its operating temperature, ohms
$S$	Instantaneous point velocity or speed in x-direction, ft/sec
$t$	Temperature at a point, $^{\circ}F$
$t_o$	Temperature of undisturbed stream, at a point $^{\circ}F$
$t_c$	Temperature at center of wake, $^{\circ}F$
$\bar{t}$	Bulk temperature, $^{\circ}F$
$T$	Absolute temperature at a point, $^{\circ}R$
$\bar{u}$	Time average of instantaneous point velocity or speed in x-direction, ft/sec
$u$	Instantaneous point velocity or speed in x-direction, ft/sec
$u_b$	Air speed at edge of wake, assumed to be in x-direction, ft/sec
$u_c$	Air speed at center of wake, assumed to be in x-direction, ft/sec
$u'$	Fluctuating point velocity component in x-direction, ft/sec
$U$	Time average of instantaneous speed at a point, ft/sec
$U$	Instantaneous speed at a point, direction unspecified, ft/sec
$\sqrt{U}$	Time average of square root of instantaneous speed at a point, ft/sec
$\bar{V}$	Time average of point velocity or speed in x-direction, ft/sec
$V$	Instantaneous point velocity or speed in x-direction, ft/sec
$V'$	Fluctuating point velocity component in x-direction, ft/sec
$\underline{W}$	Total work, B.t.u.
$x$	Longitudinal coordinate in channel with origin at centerline of cylinder, ft or in
$y$	Vertical coordinate in channel with origin at lower wall, ft or in
$z$	Lateral coordinate in channel with origin at longitudinal midline of cylinder, ft or in.

- $y'$  Vertical coordinate in channel with origin at center of wake of cylinder, ft or in
- $y'_b$  Width of wake, measured vertically, from the center to the edge of the wake
- $y'/y'_b$  Fraction of width of wake

Greek letters

- $\alpha$  Ratio of peak amplitude of velocity fluctuations to true average velocity at a point
- $\beta$  Ratio of measured average velocity to true average velocity
- $\gamma$  Angle, radians
- $\epsilon_c$  Eddy conductivity,  $\text{ft}^2/\text{sec}$
- $\epsilon_D$  Eddy diffusivity,  $\text{ft}^2/\text{sec}$
- $\epsilon_m$  Eddy viscosity,  $\text{ft}^2/\text{sec}$
- $\theta$  Time, sec
- $\kappa$  Thermometric conductivity,  $\text{ft}^2/\text{sec}$
- $\mu$  Absolute viscosity of fluid  $\text{lb sec}/\text{ft}^2$
- $\mu_f$  Absolute viscosity of fluid at arithmetic mean of wall and fluid temperature  $\text{lb sec}/\text{ft}^2$
- $\nu$  Kinematic viscosity of fluid,  $\text{ft}^2/\text{sec}$
- $\rho$  Specific mass,  $\text{lb sec}^2/\text{ft}^4$
- $\sigma$  Specific weight,  $\text{lb}/\text{ft}^3$
- $\omega$  Frequency of fluctuations, radians/sec
- $\phi$  Phase angle, radians
- $\tau_{yx}$  Stress acting in x-direction over an element of surface which is perpendicular to the y-axis,  $\text{lb}/\text{ft}^2$  or  $\text{lb}/\text{in}^2$
- $\tau_{zx}$  Stress acting in x-direction over an element of surface which is perpendicular to the z-axis,  $\text{lb}/\text{ft}^2$  or  $\text{lb}/\text{in}^2$

### Subscripts

- x      Value of quantity indicated in the positive x-direction  
y      Value of quantity indicated in the positive y-direction  
z      Value of quantity indicated in the positive z-direction

### Mathematical symbols

d      Differential of quantity indicated

D      Total differential of quantity indicated

$\frac{\partial A}{\partial B}$       Rate of change of A with respect to B, all other independent variables being held constant

## References

1. Bakhmeteff, B. A., The Mechanics of Turbulent Flow, Princeton University Press (1941).
2. Reynolds, O. S., Proc. Manchester Lit. and Phil. Soc., 14, 7 (1874).
3. Jakob, M. and Hawkins, G. A., Elements of Heat Transfer and Insulation, Wiley and Sons (1942).
4. Dryden, H. L. and Kuethe, A. M., NACA Tech. Rept. No. 320 (1929).
5. Schlichting, H., Ingenieur-Archiv, 1, 533-571 (1930).
6. Townsend, A. A., Proc. Roy. Soc., London, A190, 551-561 (1947).
7. Conings, E. W. Clapp, J. T., and Taylor, J. F., Ind. Eng. Chem., 40, 1076-1082 (1948).
8. Fage, A. and Falkner, T. P., Proc. Roy. Soc., London, A135, 702-705 (1932).
9. Goldstein, S., Modern Developments in Fluid Dynamics, I and II, Oxford University Press (1938).
10. Billman, G. W., Ph. D. Thesis, California Institute of Technology (1948).
11. Corcoran, W. H., Ph. D. Thesis, California Institute of Technology (1948).
12. Willis, J. B., Review of Hot Wire Anemometry, Australian Council for Aeronautics Report No. ACA-19 (October 1945).
13. American Inst. of Physics, Temperature, Its Measurement and Control, Reinhold (1941).
14. King, L. V., Phil. Trans. Roy. Soc., London, A214, 373 (1914).
15. Fage, A. and Johansen, F. C., Proc. Roy. Soc., London, A116, 170-397 (1927).
16. Relf, E. F. and Simmons, L. F. G., ARC Repts. and Memo., No. 917 (1924).
17. Fage, A. and Johansen, F. C., Phil. Mag., (7) 5, 417-44 (1928).
18. Wilmer, W., NACA Tech. Memo. No. 967 (1941).

19. Ray, B. B., Proc. Indian Association Cultivation Sci., 5, 95 (1920).
20. Mc Adams, W. N., Heat Transmission, McGraw-Hill (1942).
21. Lacey, W. N. and Sage, B. H., Thermodynamics of One Component Systems, California Institute of Technology (1940).
22. Prandtl, L. and Tietjens, O. G., Fundamentals of Hydro-and Aeromechanics, Mc-Graw Hill (1934).
23. Boelter, L. M. K., et. al., Heat Transfer Notes, University of California Press (1946).
24. Taylor, G. I., Pro. Roy. Soc., London, A135, 685-701 (1932).
25. N. Hu, Chinese J. Phys., 5, 1-29 (July 1944).
26. Goldstein, S., Proc. Camb. Phil. Soc., 34, 48-67 (1938).
27. Dryden, H. L., Schubauer, G. B., Mock, W. C., and Skramstad, H. K., NACA Tech. Rept. No. 581 (1937).
28. Schubauer, G. B., NACA Tech. Rept. No. 524 (1935).
29. Mock, W. C., Jr. and Dryden, H. L., NACA Tech. Rept. No. 448 (1933).

## LIST OF FIGURES

1. Various Types of Transfers in Turbulent Gas Streams
2. General Layout of Equipment
3. Stainless Steel Cylinder Mounted in Channel
4. Brass Cylinder Mounted in Channel
5. Pitot Tube and Thermanemometer
6. Thermanemometer Electrical Circuit
7. Thermanemometer Air Speed Calibration Curve
8. Magnitude of Error in Air Speed Measurement due to Amplitude of Air Speed Fluctuations
9. Velocity Measurements Made with Compensated Circuit
10. Temperature Distribution in Wake of Heated Steel Cylinder at Bulk Air Velocity of 6.99 ft./sec.
11. Temperature Field in Wake of Heated Steel Cylinder at Bulk Air Velocity of 6.99 ft./sec.
12. Temperature Distribution in Wake of Heated Steel Cylinder at Bulk Air Velocity of 12.7 ft./sec.
13. Temperature Field in Wake of Heated Steel Cylinder at Bulk Air Velocity of 12.7 ft./sec.
14. Photograph of Temperature Field in Wake of Heated Cylinder (19)
15. Temperature Distribution in Wake of Heated Steel Cylinder at Bulk Air Velocity of 24.8 ft./sec.
16. Temperature Distribution in Wake of Heated Steel Cylinder at Bulk Air Velocity of 24.8 ft./sec.
17. Temperature Distribution in Wake of Heated Steel Cylinder at Bulk Air Velocity of 24.8 ft./sec.
18. Temperature Field in Wake of Heated Steel Cylinder at Bulk Air Velocity of 24.8 ft./sec.
19. Temperature Distribution in Wake of Heated Steel Cylinder at Bulk Air Velocity of 24.8 ft./sec.

20. Temperature Distribution in Wake of Heated Steel Cylinder at Bulk Air Velocity of 44.7 ft./sec.
21. Temperature Field in Wake of Heated Steel Cylinder at Bulk Air Velocity of 44.7 ft./sec.
22. Temperature at Center of Wake versus (Distance Downstream)<sup>-1/2</sup>
23. Width of Wake versus Distance Downstream
24. Circumferential Temperature Distribution on Surface of Cylinder at a Bulk Air Velocity of 14.4 ft./sec.
25. Circumferential Temperature Distribution on Surface of Cylinder at a Bulk Air Velocity of 23.8 ft./sec.
26. Rate of Thermal Energy Transfer from Cylinder versus Surface Temperature
27. Nusselt Number versus Reynolds Number
28. Air Speed Distribution in Wake of Heated Steel Cylinder at Bulk Air Velocity of 6.99 ft./sec.
29. Air Speed Field in Wake of Heated Steel Cylinder at Bulk Air Velocity of 6.99 ft./sec.
30. Air Speed Distribution in Wake of Heated Steel Cylinder at Bulk Air Velocity of 12.7 ft./sec.
31. Air Speed Field in Wake of Heated Steel Cylinder at Bulk Air Velocity of 12.7 ft./sec.
32. Air Speed Distribution in Wake of Heated Steel Cylinder at Bulk Air Velocity of 24.8 ft./sec.
33. Air Speed Field in Wake of Heated Steel Cylinder at Bulk Air Velocity of 24.8 ft./sec.
34. Air Speed Distribution in Wake of Heated Steel Cylinder at Bulk Air Velocity of 44.7 ft./sec.
35. Air Speed Field in Wake of Heated Steel Cylinder at Bulk Air Velocity of 44.7 ft./sec.
36. Air Speed Distribution in Wake of Steel Cylinder at Bulk Air Velocity of 44.7 ft./sec.
37. Values of Eddy Viscosity and Eddy Conductivity in Wake of Heated Cylinder
38. Comparison of Theories of Turbulence at Bulk Air Velocity of 6.99 ft./sec.



39. Comparison of Theories of Turbulence at Bulk Air Velocity of 12.7 ft./sec.
40. Comparison of Theories of Turbulence at Bulk Air Velocity of 24.8 ft./sec.
41. Comparison of Theories of Turbulence at Bulk Air Velocity of 44.7 ft./sec.
42. Correlation of Temperature and Velocity Distribution in Wake at Bulk Air Velocity of 44.7 ft./sec.

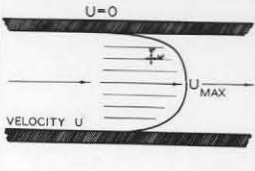
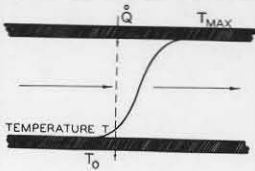
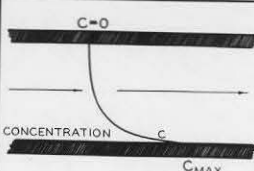
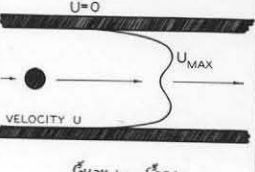
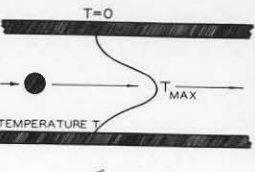
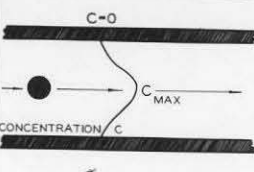
	MOMENTUM TRANSFER	HEAT TRANSFER	MASS TRANSFER
UNIFORM TWO DIMENSIONAL FLOW	 $\tau = K_c (V + \epsilon_m) \frac{du}{dy}$	 $\frac{\dot{Q}}{\tau} = K_c (K + \epsilon_h) \frac{dT}{dy}$	 $M = K_c (D + \epsilon_m) \frac{dc}{dy}$
NON UNIFORM TWO DIMENSIONAL FLOW	 $\epsilon_m = \frac{\int_0^y U \frac{\partial U}{\partial y} dy + \int_0^y \frac{\partial U}{\partial y} dy}{\rho \frac{\partial U}{\partial y}} - \nu$	 $\epsilon_h = \frac{\int_0^y T \frac{\partial T}{\partial y} dy}{\rho c_p \frac{\partial T}{\partial y}} - K$	 $\epsilon_m = \frac{\int_0^y C \frac{\partial C}{\partial y} dy}{\rho \frac{\partial C}{\partial y}} - D$

Figure 1. Various Types of Transfers in Turbulent Gas Streams

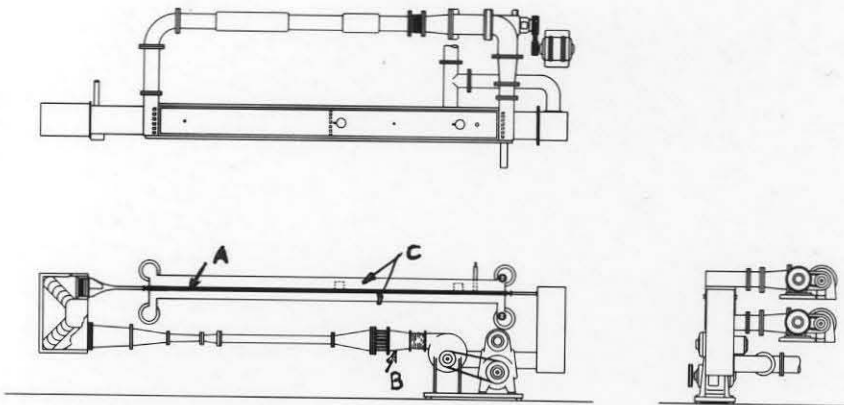


Figure 2. General Layout of Equipment

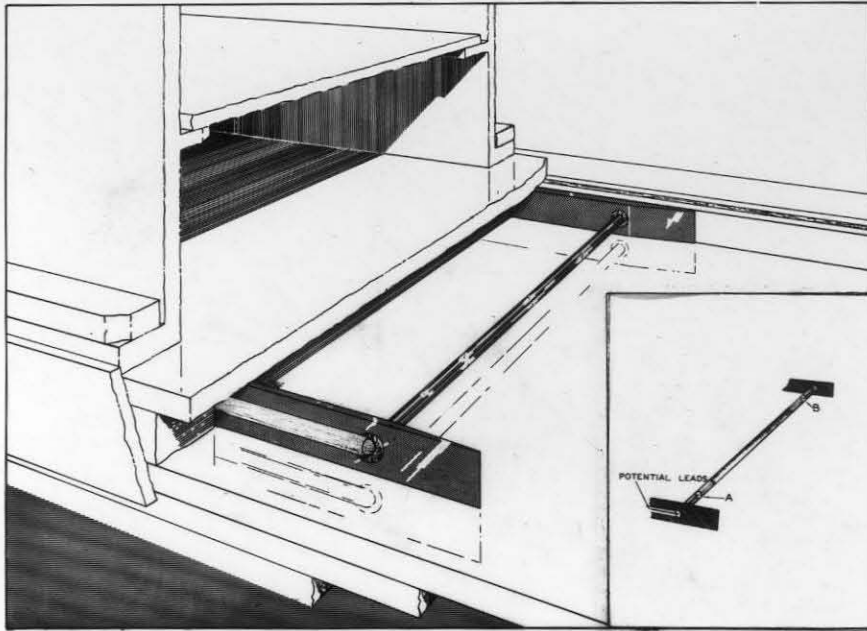


Figure 3. Stainless Steel Cylinder Mounted in Channel

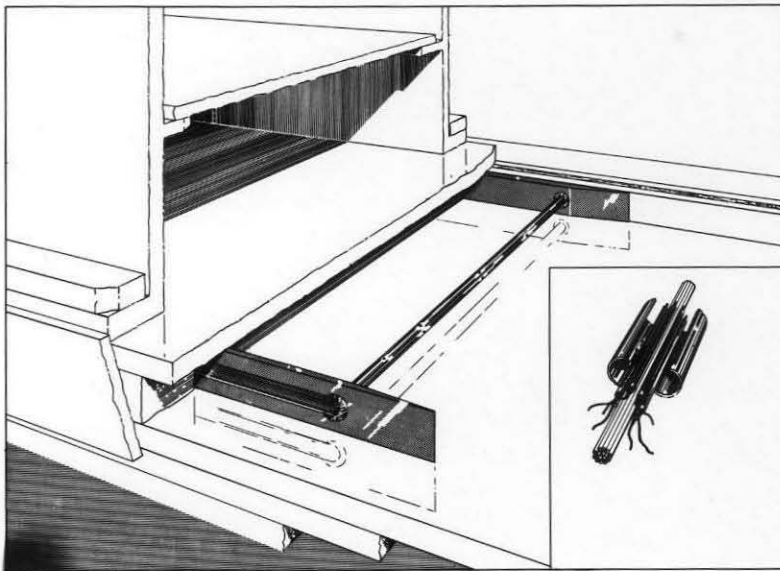


Figure 4. Brass Cylinder Mounted in Channel

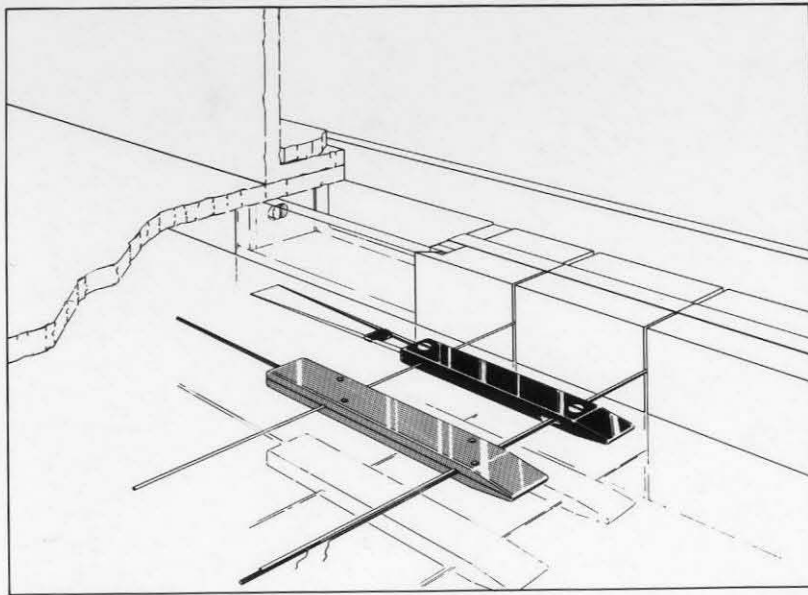


Figure 5. Pitot Tube and Thermanemometer

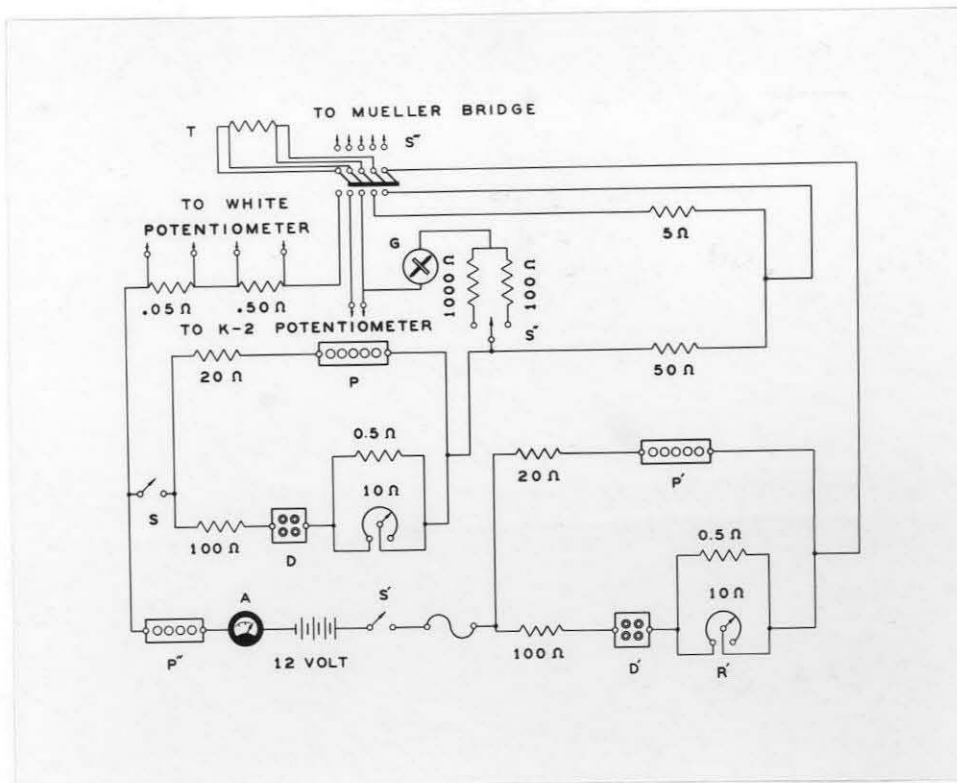


Figure 6. Thermanemometer Electrical Circuit

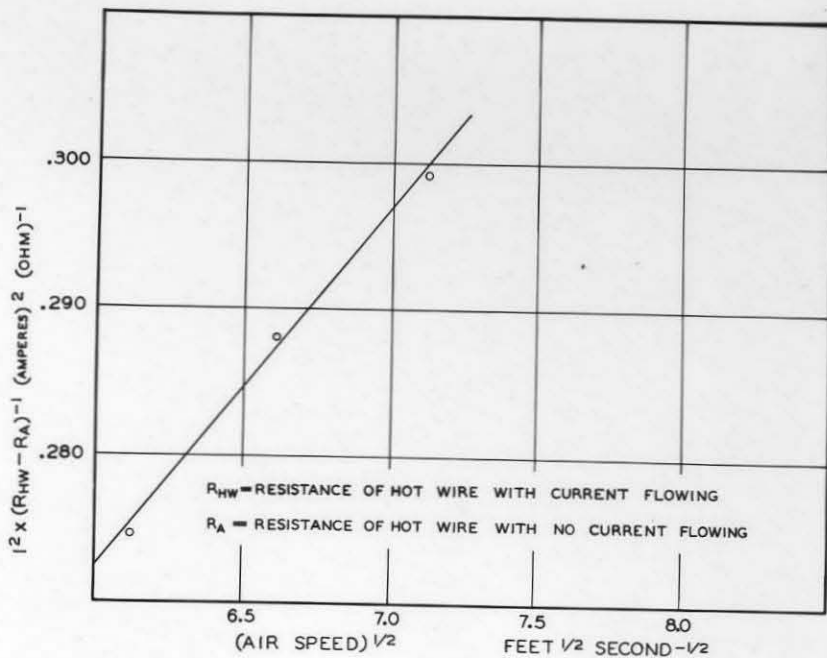


Figure 7. Thermanemometer Air Speed Calibration Curve

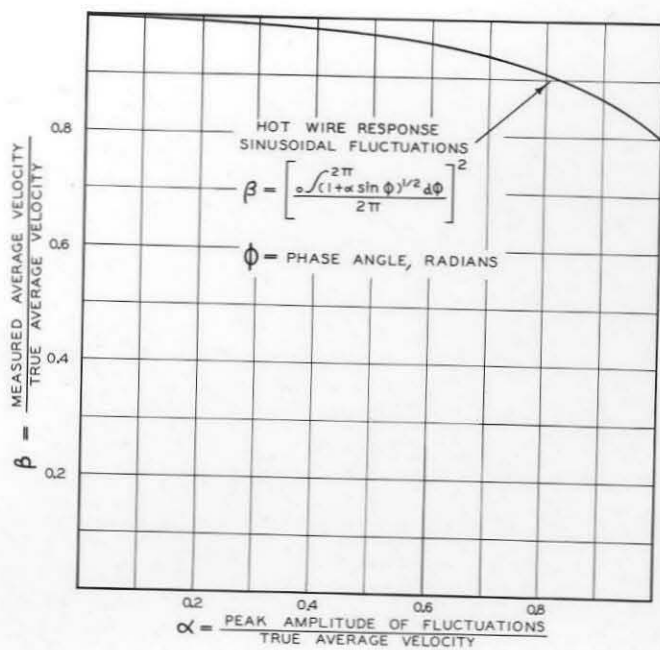


Figure 8. Magnitude of Error in Air Speed Measurement Due to Amplitude of Air Speed Fluctuations

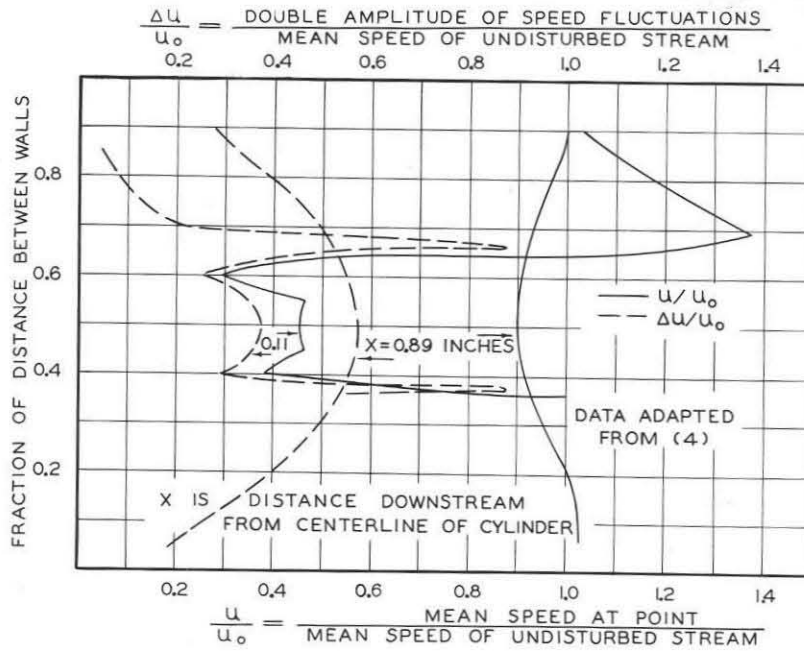


Figure 9. Velocity Measurements Made with Compensated Circuit

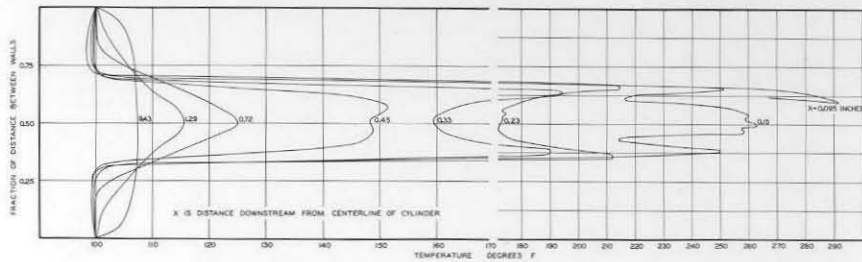


Figure 10. Temperature Distribution in Wake of Heated Steel Cylinder at Bulk Air Velocity of 6.99 ft./sec.

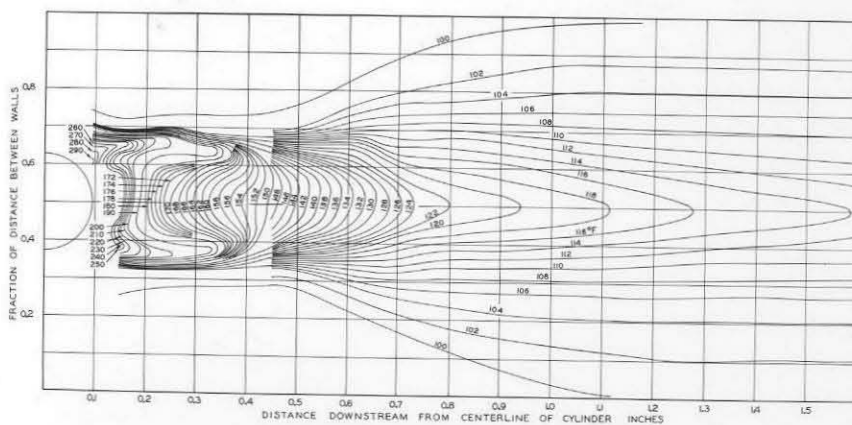


Figure 11. Temperature Field in Wake of Heated Steel Cylinder at Bulk Air Velocity of 6.99 ft./ sec.

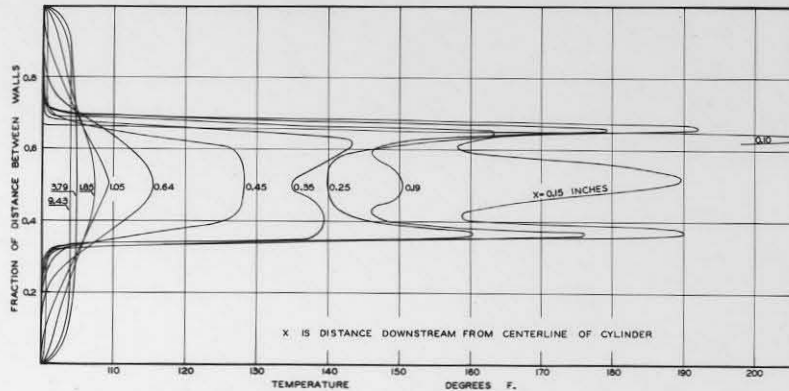


Figure 12. Temperature Distribution in Wake of Heated Steel Cylinder at Bulk Air Velocity of 12.7 ft./sec.

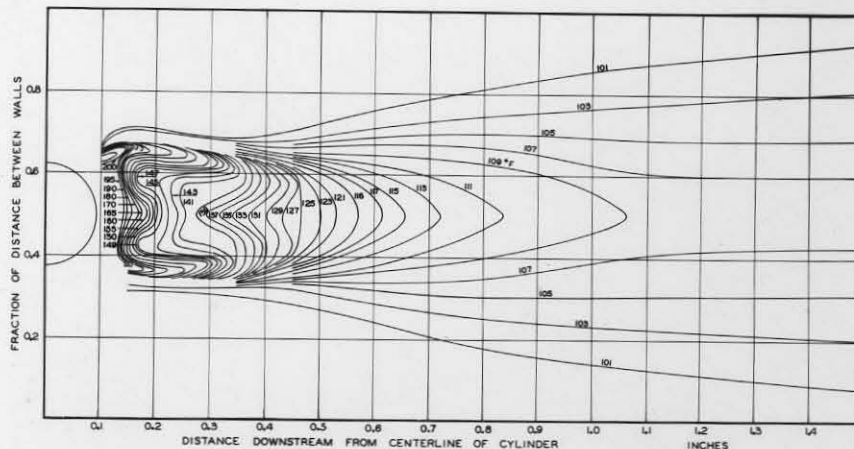


Figure 13. Temperature Field in Wake of Heated Steel Cylinder at Bulk Air Velocity of 12.7 ft./sec.



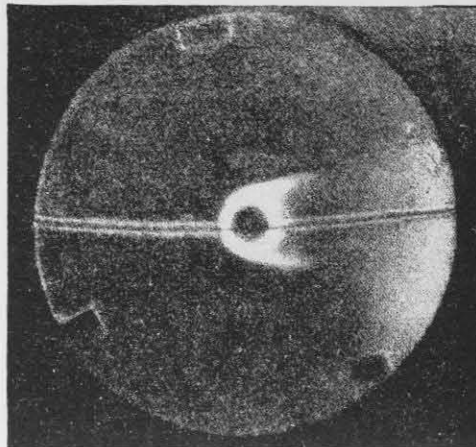


Figure 14. Photograph of Temperature Field  
in Wake of Heated Cylinder

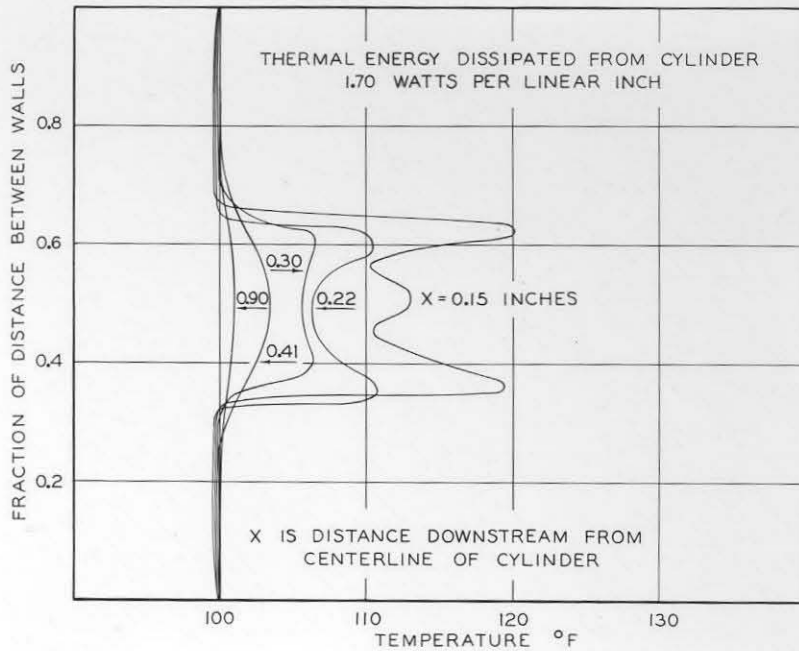


Figure 15. Temperature Distribution in Wake of Heated Steel Cylinder at Bulk Air Velocity of 24.8 ft./ sec.

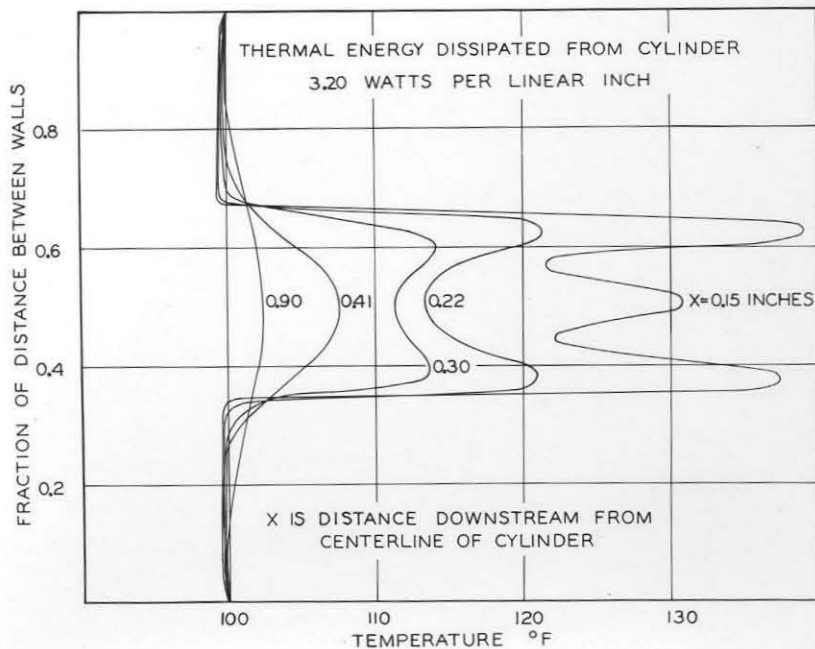


Figure 16. Temperature Distribution in Wake of Heated Steel Cylinder at Bulk Air Velocity of 24.8 ft./sec.

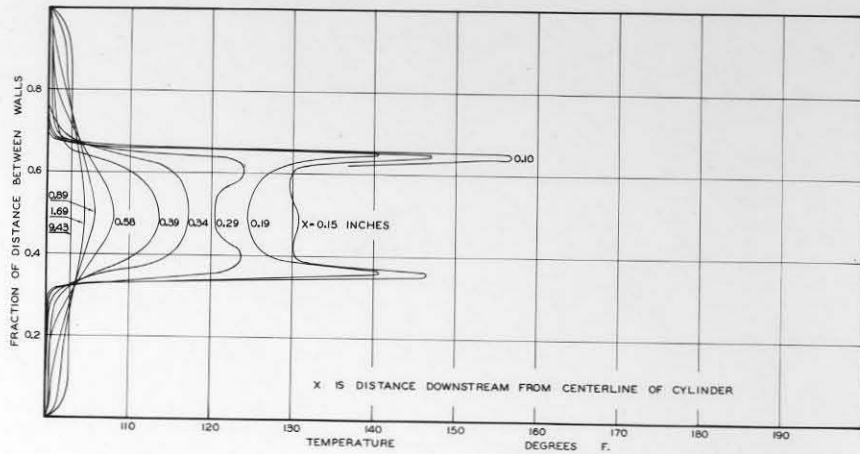
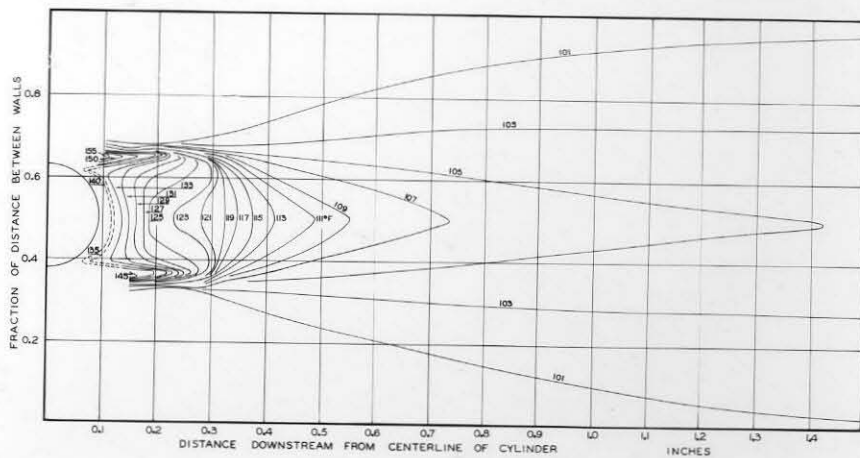


Figure 17. Temperature Distribution in Wake of Heated Steel Cylinder at Bulk Air Velocity of 24.8 ft./sec.



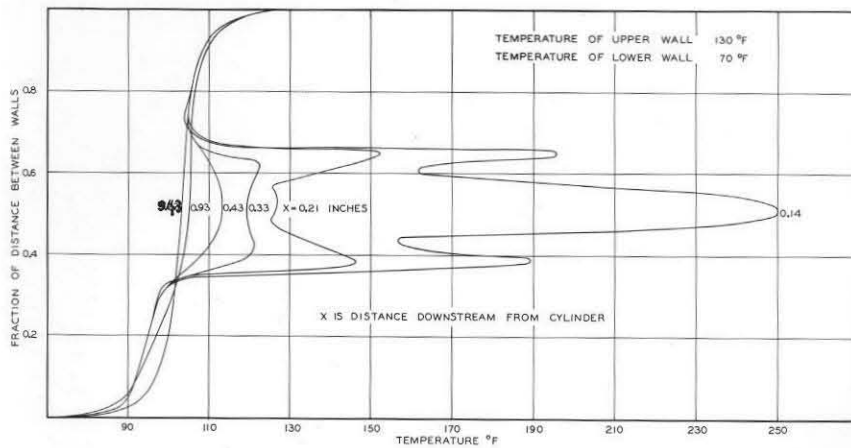


Figure 19. Temperature Distribution in Wake of Heated Steel Cylinder at Bulk Air Velocity of 24.8 ft./sec.

Figure 21. Temperature Field in Wake of Heated Steel Cylinder at Bulk Air Velocity of 44.7 ft./sec.

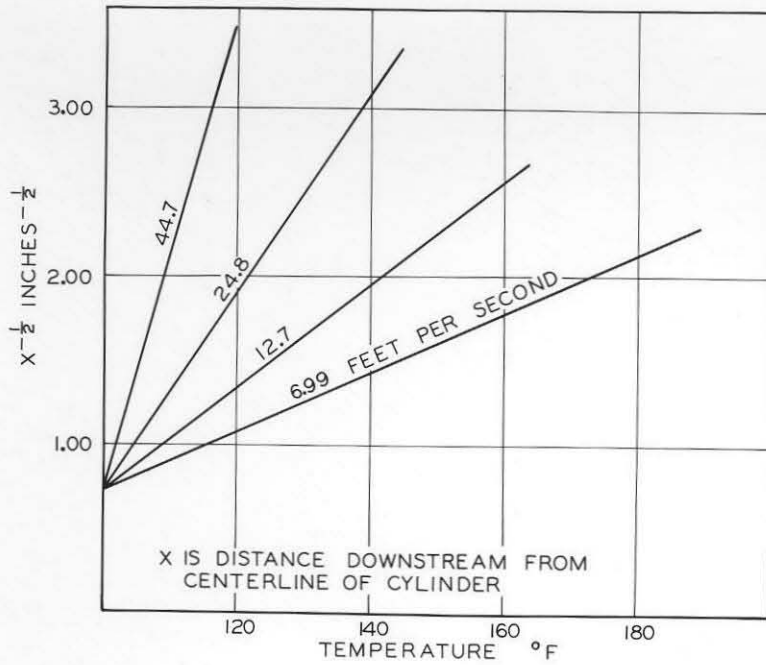


Figure 22. Temperature at Center of Wake  $X^{1/2}$  versus (Distance Downstream)  $X^{1/2}$

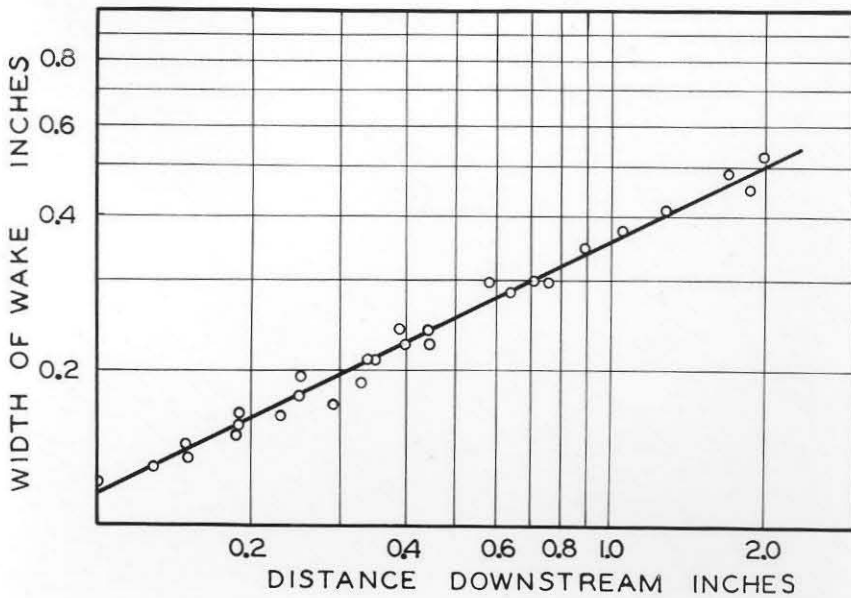


Figure 23. Width of Wake versus Distance Downstream

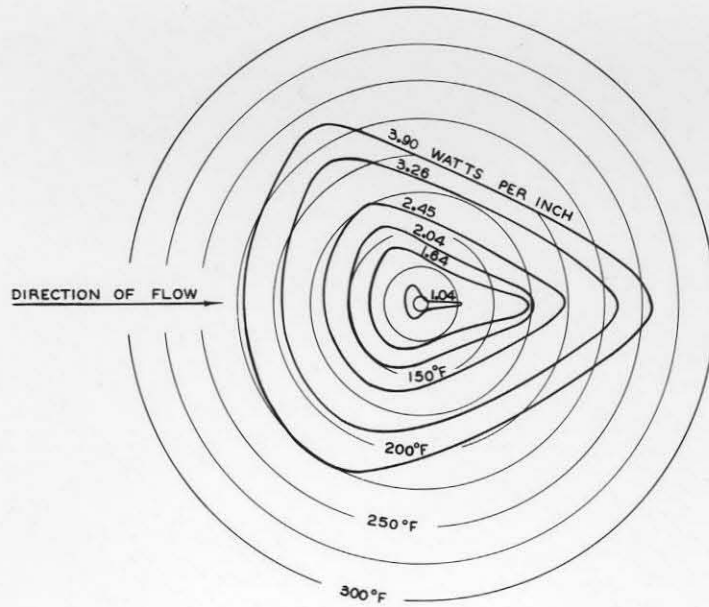


Figure 24. Circumferential Temperature Distribution on Surface of Cylinder at a Bulk Air Velocity of 14.4 ft./sec.

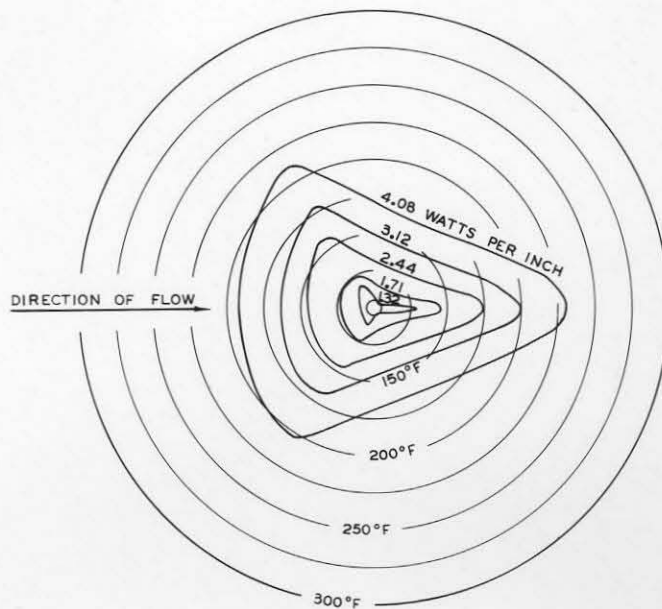


Figure 25. Circumferential Temperature Distribution on Surface of Cylinder at a Bulk Air Velocity of 23.8 ft./sec.

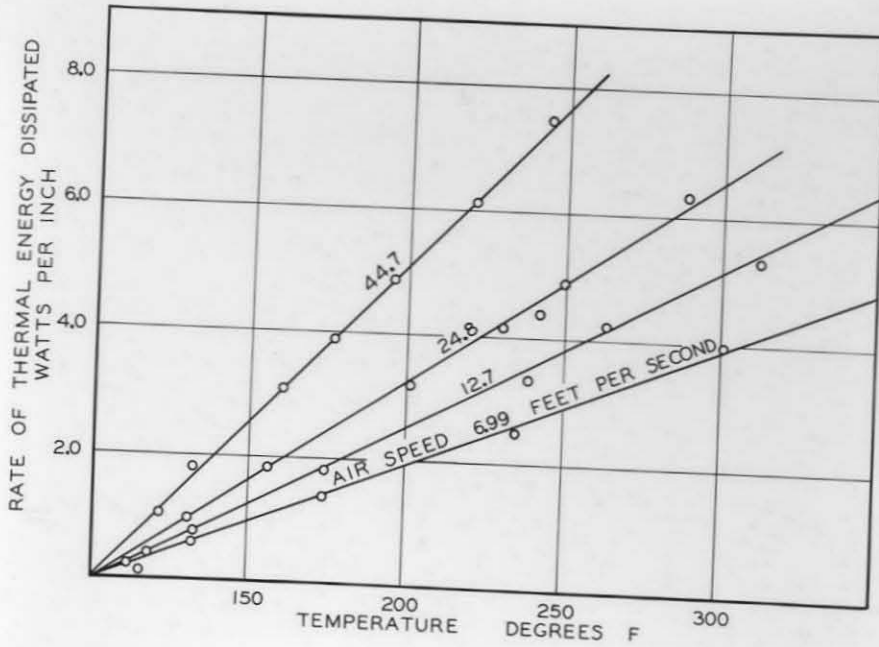


Figure 26. Rate of Thermal Energy Transfer from Cylinder versus Surface Temperature

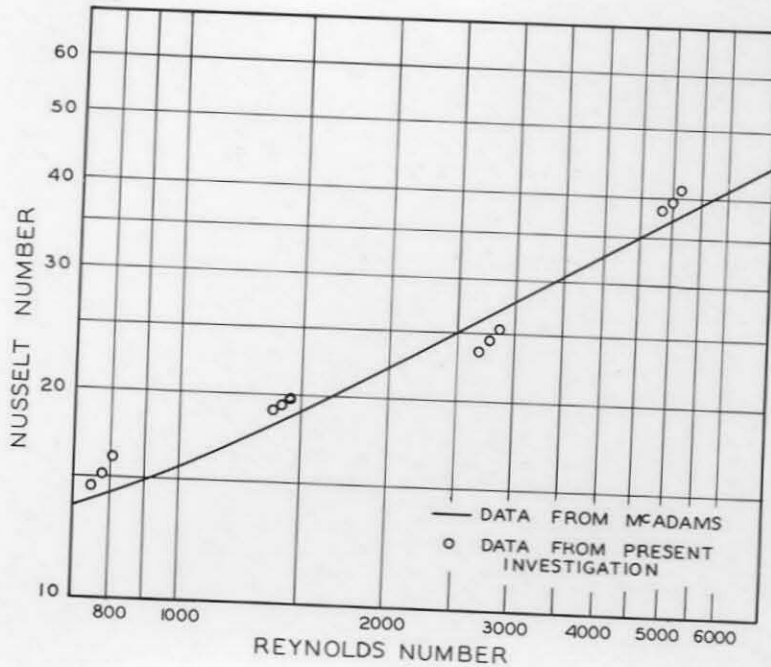


Figure 27. Nusselt Number versus Reynolds Number



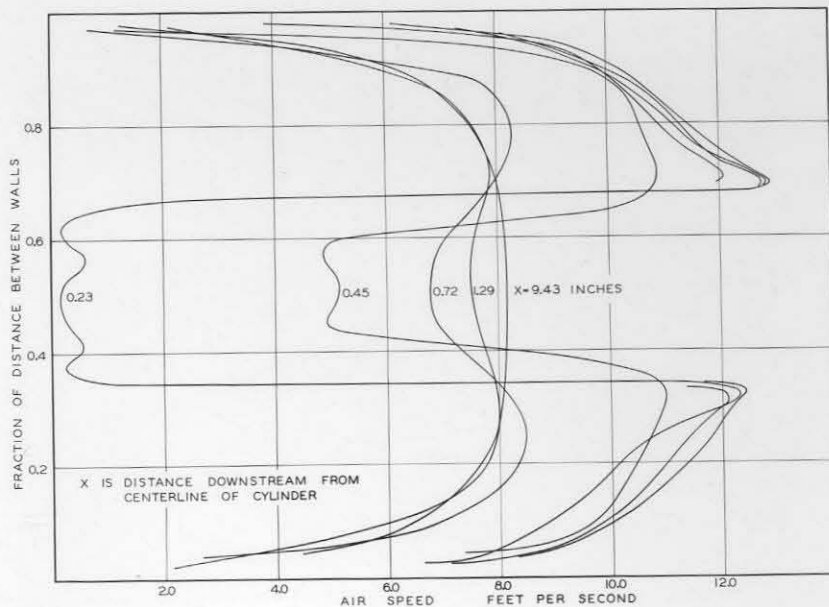


Figure 28. Air Speed Distribution in Wake of Heated Steel Cylinder at Bulk Air Velocity of 6.99 ft./sec.

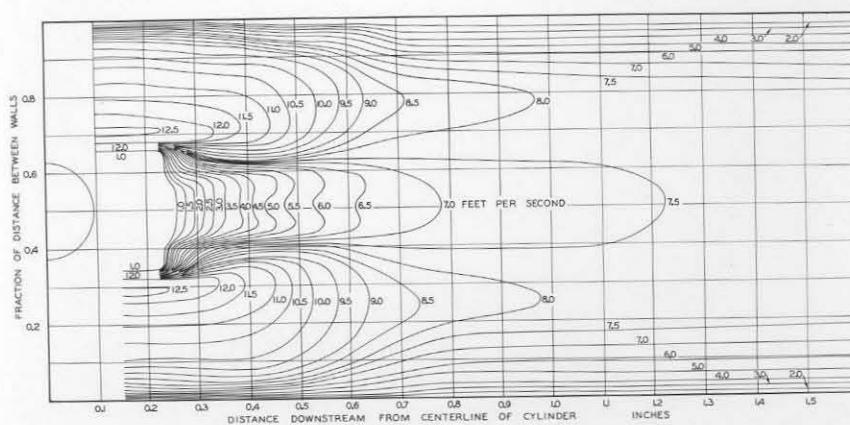


Figure 29. Air Speed Field in Wake of Heated Steel Cylinder at Bulk Air Velocity of 6.99 ft./sec.



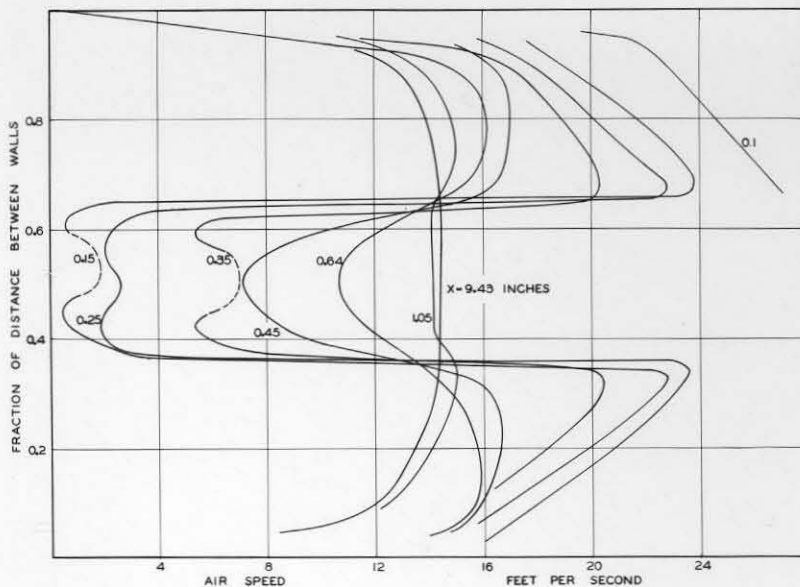


Figure 30. Air Speed Distribution in Wake of Heated Steel Cylinder at Bulk Air Velocity of 12.7 ft./sec.

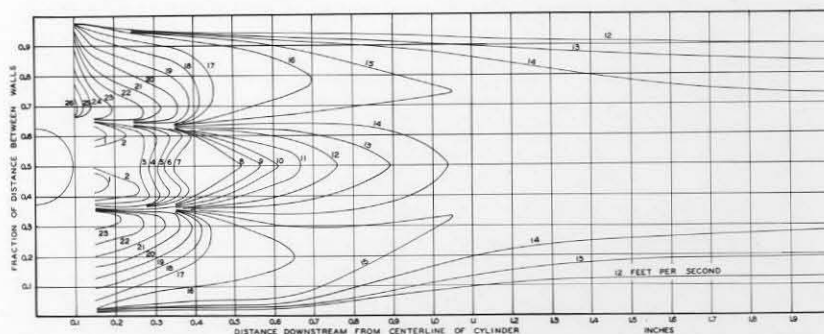


Figure 31. Air Speed Field in Wake of Heated Steel Cylinder at Bulk Air Velocity of 12.7 ft./sec.

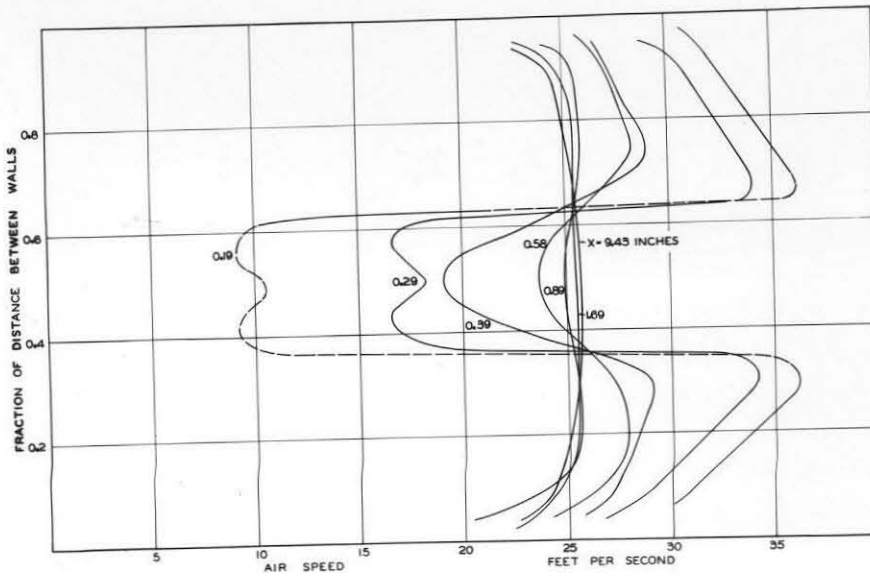


Figure 32. Air Speed Distribution in Wake of Heated Steel Cylinder at Bulk Air Velocity of 24.8 ft./sec.

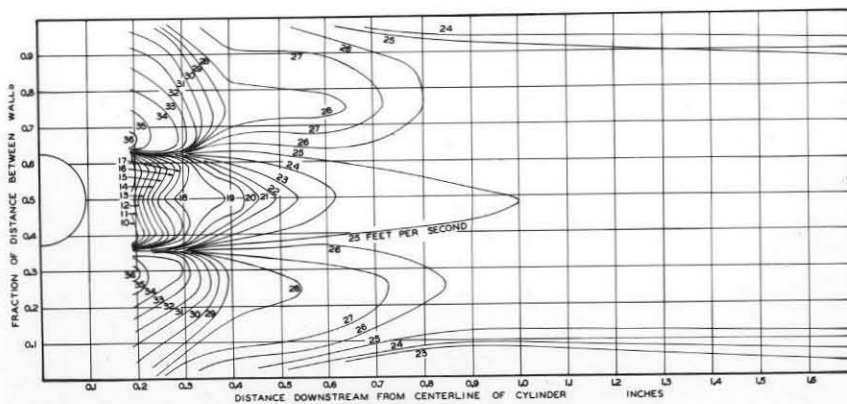


Figure 33. Air Speed Field in Wake of Heated Steel Cylinder at Bulk Air Velocity of 24.8 ft./sec.

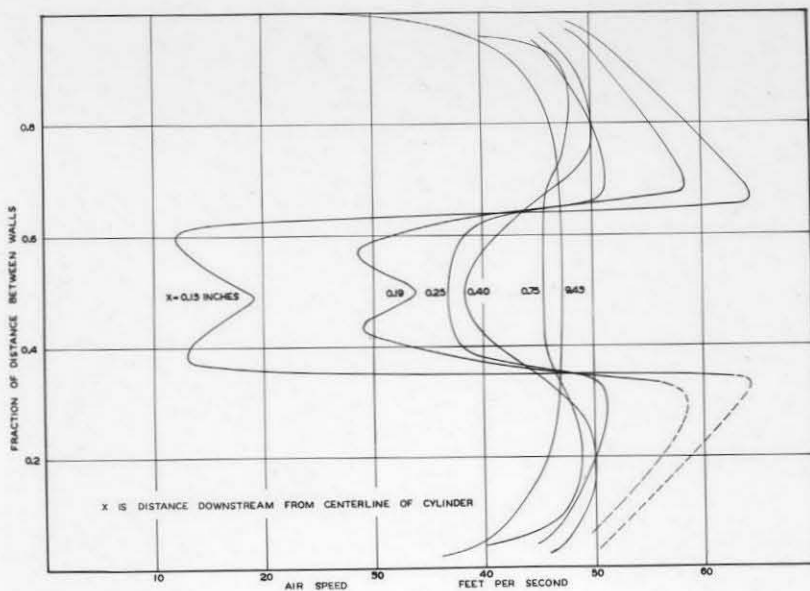


Figure 34. Air Speed Distribution in Wake of Heated Steel Cylinder at Bulk Air Velocity of 44.7 ft./sec.

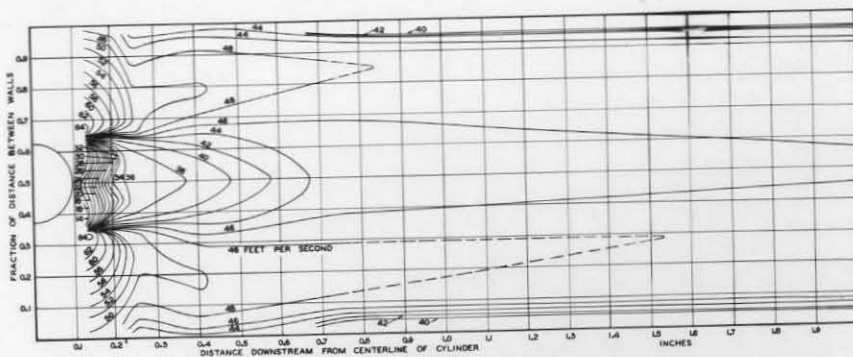


Figure 35. Air Speed Field in Wake of Heated Steel Cylinder at Bulk Air Velocity of 44.7 ft./sec.

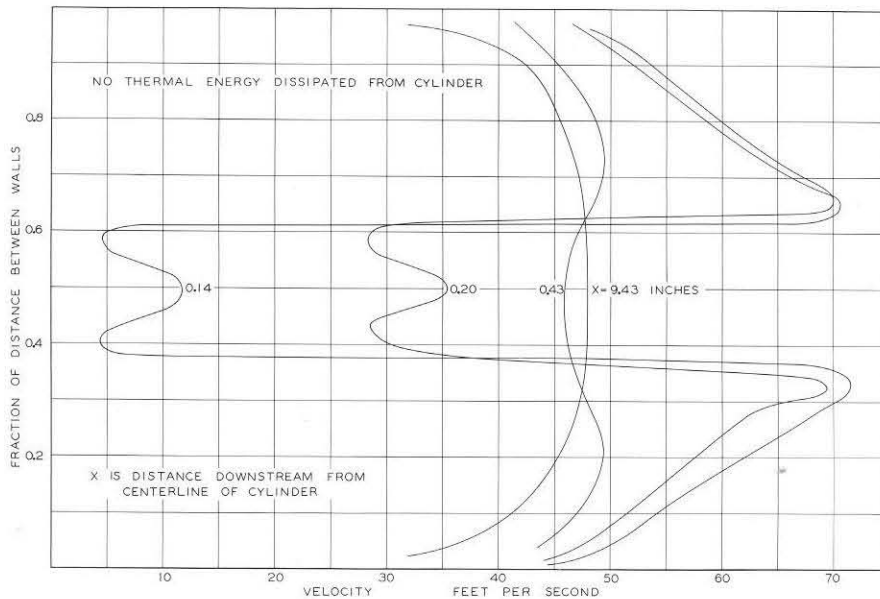


Figure 36. Air Speed Distribution in Wake of Heated Steel Cylinder at Bulk Air Velocity of 44.7 ft./sec.



Figure 37. Comparison of Theories of Turbulence at Bulk Air Velocity of 4.29 ft./sec.

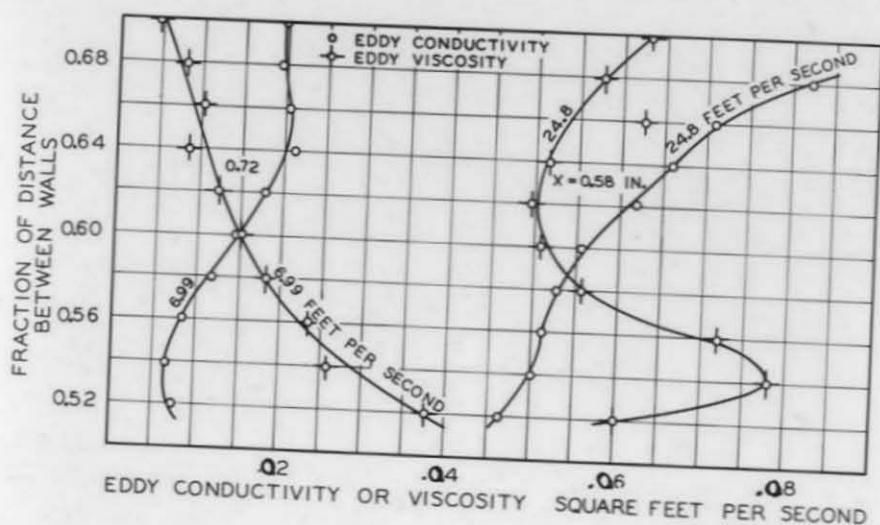


Figure 37. Values of Eddy Viscosity and Eddy Conductivity in Wake of Heated Cylinder

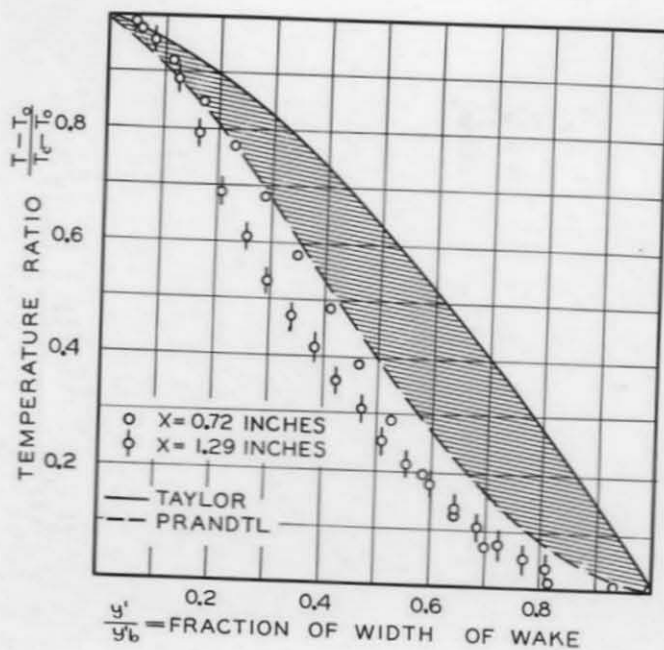


Figure 38. Comparison of Theories of Turbulence at Bulk Air Velocity of 6.99 ft./sec.

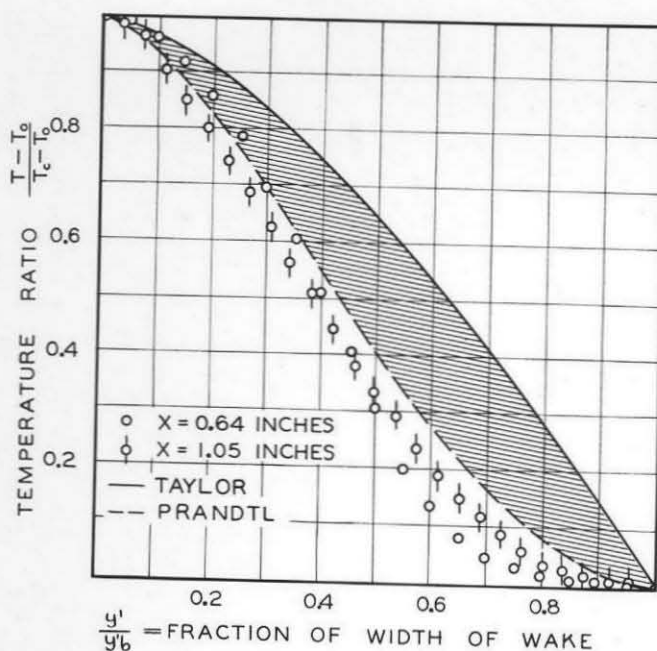


Figure 39. Comparison of Theories of Turbulence at Bulk Air Velocity of 12.7 ft./sec.

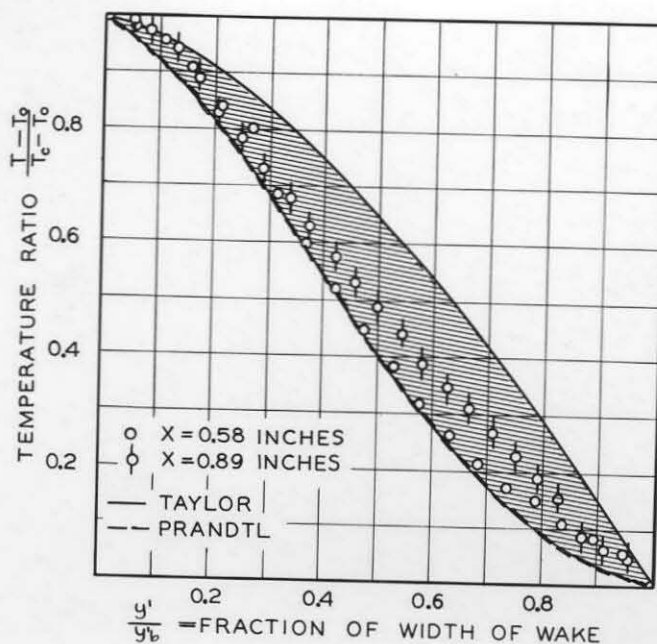


Figure 40. Comparison of Theories of Turbulence at Bulk Air Velocity of 24.8 ft./sec.

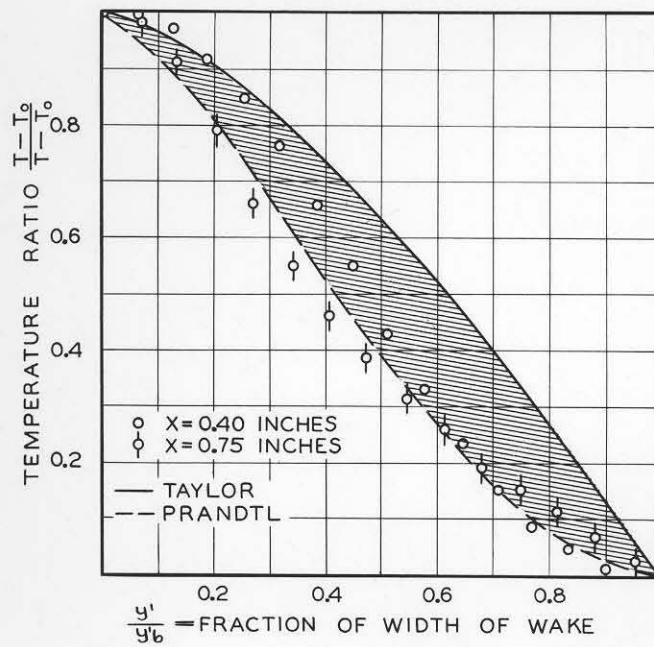


Figure 41. Comparison of Theories of Turbulence at Bulk Air Velocity of 44.7 ft./sec.

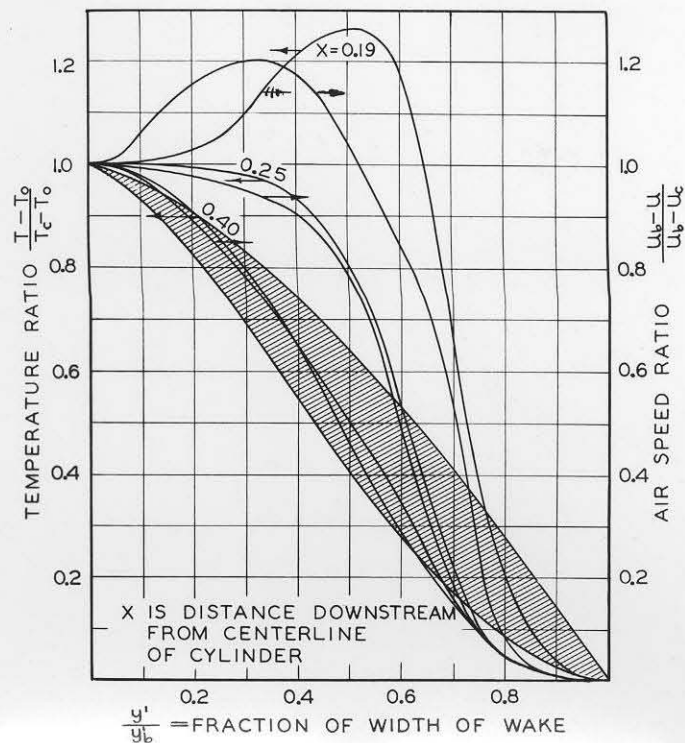


Figure 42. Correlation of Temperature and Velocity Distribution in Wake at Bulk Velocity of 44.7 ft./sec.

LIST OF TABLES

- I. Temperature and Air Speed Distribution in the Wake of a Heated Steel Cylinder
- II. Circumferential Temperature Distribution on the Surface of a Heated Brass Cylinder
- III. Thermal Energy Transfer as a Function of Average Surface Temperature of Cylinder
- IV. Eddy Conductivity and Eddy Viscosity in the Wake of a Heated Cylinder
- V. Theoretical Correlations of Temperature and Velocity Distribution in the Wake of a Heated Cylinder



Table I. Temperature and Air Speed Distribution  
in the Wake of a Heated Steel Cylinder

Part 1.\*

Temperature Distribution					
$y/y_o^a$	$t_{oF.}^b$	$y/y_o$	$t_{oF.}$	$y/y_o$	$t_{oF.}$
$x^c = 0$ in.		0.625	267.17	0.062	99.55
$y_o^d = 0.747$ in.		0.639	268.69	0.115	99.70
0.652	274.50	0.652	265.27	0.169	99.37
0.705	100.40	0.679	148.58	0.223	99.75
0.759	99.60	0.692	106.93	0.276	99.55
0.813	99.60	0.705	101.16	0.303	99.93
0.866	99.65	0.732	100.30	0.330	112.09
0.920	99.70	0.759	99.86	0.343	142.65
0.960	99.85	0.786	99.70	0.357	209.67
0.983	99.95	0.839	99.70	0.370	237.90
		0.893	99.70	0.383	249.69
$x = 0.13$ in.		0.946	99.84	0.397	236.00
$y_o = 0.747$ in.		0.969	100.08	0.410	228.02
0.558	334.07			0.429	213.96
0.585	318.10	$x = 0.15$ in.		0.442	218.52
0.598	291.27	$y_o = 0.746$ in.		0.456	246.27
0.610	269.76	0.036	99.75		

\* Bulk velocity - 6.99 ft./sec.  
Reynolds number based on channel cross section - 4270  
Reynolds number based on cylinder - 562  
Average Temperature of cylinder - 368.2°F.  
Rate of dissipation of thermal energy - 5.42 watts/in.

<sup>a</sup> Fraction of distance between walls  
<sup>b</sup> Air stream temperature corrected for impact effect  
<sup>c</sup> Distance downstream from centerline of cylinder  
<sup>d</sup> Distance between walls

Table I, Part 1 (cont'd.)

Temperature Distribution

$y/y_0$	$t_{OF.}$	$y/y_0$	$t_{OF.}$	$y/y_0$	$t_{OF.}$
$x = 0.15$ in.		0.893	98.41	0.531	173.29
$y_0 = 0.746$ in.		0.946	98.79	0.545	174.43
0.469	258.05	0.976	100.01	0.558	173.06
0.483	257.29	$x = 0.23$ in.		0.572	176.86
0.496	262.61			0.585	177.56
0.517	258.81	$y_0 = 0.747$ in.		0.598	180.15
0.531	258.80	0.033	100.08	0.612	182.43
0.544	259.57	0.063	99.78	0.625	190.48
0.558	253.56	0.116	99.89	0.639	201.79
0.571	251.97	0.170	99.67	0.652	213.88
0.584	242.09	0.224	99.79	0.665	213.58
0.598	218.52	0.264	99.58	0.679	190.17
0.611	216.24	0.304	100.39	0.692	145.69
0.625	223.08	0.331	117.87	0.705	105.27
0.638	239.04	0.344	169.87	0.732	99.86
0.651	250.83	0.357	212.06	0.786	99.73
0.665	228.02	0.371	210.92	0.839	99.75
0.678	174.96	0.384	199.14	0.893	99.81
0.692	117.11	0.411	189.33	0.933	99.86
0.705	99.78	0.424	178.84	0.961	100.04
0.732	98.71	0.451	173.67		
0.786	98.18	0.478	171.77		
0.839	98.46	0.518	173.21		

Table I, Part 1 (cont'd.)

Temperature Distribution

$y/y_o$	$t_{o_F.}$	$y/y_o$	$t_{o_F.}$	$y/y_o$	$t_{o_F.}$
$x = 0.38 \text{ in.}$		0.649	174.81	0.628	142.20
$y_o = 0.740 \text{ in.}$		0.676	120.91	0.681	106.89
0.024	99.70	0.703	100.96	0.734	100.01
0.054	99.55	0.757	99.40	0.788	99.63
0.108	99.43	0.811	99.32	0.837	99.63
0.162	99.40	0.865	99.48	0.894	99.60
0.216	99.40	0.919	99.48	0.947	99.82
0.270	99.44	0.946	99.61	0.969	77.18
0.324	114.37	0.979	99.92		
0.351	161.13			$x = 0.72 \text{ in.}$	
0.365	178.99	$x = 0.45 \text{ in.}$		$y_o = 0.756 \text{ in.}$	
0.378	180.13	$y_o = 0.753 \text{ in.}$		0.038	100.22
0.398	176.71	0.044	99.70	0.127	99.86
0.419	167.21	0.097	99.40	0.193	100.24
0.449	163.03	0.150	99.40	0.259	103.20
0.478	160.75	0.203	99.40	0.325	109.49
0.500	159.61	0.256	99.52	0.392	115.50
0.527	159.61	0.309	100.54	0.458	121.93
0.554	161.51	0.363	118.25	0.524	124.67
0.581	164.93	0.416	146.00	0.590	119.92
0.608	172.91	0.469	148.73	0.656	114.18
0.622	180.13	0.522	148.40	0.722	107.61
0.635	182.03	0.575	151.32	0.788	102.32

Table I, Part 1 (cont'd.)

Temperature Distribution

$y/y_o$	$t_{o_F}$	$y/y_o$	$t_{o_F}$
$x = 0.72$ in.		0.946	100.84
$y_o = 0.756$ in.		0.973	100.54
0.854	100.16	$x = 9.43$ in.	
0.907	100.13	$y_o = 0.736$ in.	
0.947	100.24	0.049	104.18
0.967	100.46	0.117	105.71
$x = 1.29$ in.		0.185	105.54
$y_o = 0.746$ in.		0.253	106.99
0.021	100.31	0.321	107.17
0.048	100.46	0.389	107.30
0.115	101.45	0.457	107.38
0.182	103.20	0.524	107.30
0.249	105.33	0.592	107.29
0.316	107.38	0.660	107.30
0.383	110.50	0.728	106.85
0.450	114.37	0.796	106.56
0.517	115.67	0.864	105.89
0.584	113.69	0.918	104.83
0.654	109.51	0.946	104.05
0.718	106.93	0.976	102.35
0.786	104.72		
0.853	103.05		
0.920	101.30		

Table I, Part 1 (cont'd.)

Air Speed Distribution

$y/y_0$	Air Speed (ft./sec.)	$y/y_0$	Air Speed (ft./sec.)	$y/y_0$	Air Speed (ft./sec.)
$x = 0.13$ in.		0.946	9.11	0.961	8.16
$y_0 = 0.747$ in.		0.976	6.45		
0.679	12.56			$x = 0.33$ in.	
0.732	12.19	$x = 0.23$ in.		$y_0 = 0.740$ in.	
0.786	11.28	$y_0 = 0.747$ in.		0.024	7.12
0.839	10.67	0.033	7.47	0.054	9.04
0.893	9.97	0.063	29.59	0.108	10.03
0.946	8.53	0.116	31.26	0.162	10.66
0.969	7.33	0.170	9.90	0.216	11.14
		0.224	10.40	0.270	11.64
$x = 0.15$ in.		0.304	12.28	0.324	12.81
$y_0 = 0.746$ in.		0.411	0.57	0.703	12.07
0.036	8.34	0.451	0.30	0.757	11.37
0.062	9.30	0.518	0.23	0.811	10.82
0.115	10.33	0.572	0.60	0.865	10.28
0.169	10.96	0.625	0.18	0.919	9.51
0.223	11.59	0.679	7.73	0.946	8.46
0.276	11.99	0.705	12.70	0.979	4.28
0.330	14.40	0.732	12.02		
0.678	10.80	0.786	11.41	$x = 0.45$ in.	
0.732	12.33	0.839	10.92	$y_0 = 0.753$ in.	
0.786	11.42	0.893	10.11	0.044	7.39
0.839	10.98	0.933	8.98	0.097	9.59
0.893	10.22				

Table I, Part 1 (cont'd.)

Air Speed Distribution

$y/y_0$	Air Speed (ft./sec.)	$y/y_0$	Air Speed (ft./sec.)	$y/y_0$	Air Speed (ft./sec.)
$x = 0.45$ in. $y_0 = 0.753$ in.		0.193	8.30	0.383	7.79
0.150	10.15	0.259	8.43	0.450	7.68
0.203	10.42	0.325	8.08	0.517	7.51
0.256	10.76	0.392	7.47	0.584	7.66
0.309	10.98	0.458	6.84	0.651	7.70
0.363	10.39	0.524	6.90	0.718	7.84
0.416	6.82	0.590	7.03	0.786	7.59
0.469	5.18	0.656	7.62	0.853	7.04
0.522	5.05	0.722	8.06	0.920	5.11
0.575	4.86	0.788	8.20	0.946	3.89
0.628	7.96	0.854	7.92	0.973	2.27
0.681	10.79	0.907	6.13	$x = 9.43$ in. $y_0 = 0.736$ in.	
0.734	10.87	0.947	3.41	0.049	4.77
0.788	10.57	0.967	1.15	0.117	6.79
0.837	10.43	$x = 1.29$ in. $y_0 = 0.746$ in.		0.185	7.50
0.894	9.73	0.021	2.20	0.253	7.91
0.947	7.08	0.048	3.71	0.321	8.02
0.969	1.55	0.115	6.55	0.389	8.10
$x = 0.72$ in. $y_0 = 0.756$ in.		0.182	7.66	0.457	8.14
0.038	2.79	0.249	7.93	0.524	8.11
0.127	7.51	0.316	7.95	0.592	8.07

Table I, Part 1 (cont'd.)

Air Speed Distribution

$r/y_0$  Air Speed  
(ft./sec.)

$x = 9.43$  in.

$y_0 = 0.736$  in.

0.660 8.05

0.728 7.87

0.796 7.55

0.864 6.88

0.918 5.57

0.946 4.31

0.976 1.56

Table I, Part 2\*

Temperature Distribution

$y/y_0$	$t_{\text{°F.}}$	$y/y_0$	$t_{\text{°F.}}$	$y/y_0$	$t_{\text{°F.}}$
$x = 0.10 \text{ in.}$		0.338	110.09	0.635	162.69
$y_0 = 0.740 \text{ in.}$		0.351	143.40	0.649	176.96
0.622	198.36	0.365	183.91	0.662	192.14
0.635	205.93	0.378	188.56	0.676	173.22
0.649	179.80	0.392	170.85	0.689	122.28
0.662	127.10	0.419	158.30	0.703	102.20
0.676	100.00	0.432	160.64	0.730	100.53
0.730	99.75	0.460	169.39	0.784	100.53
0.784	99.75	0.486	181.61	0.838	100.29
0.838	99.69	0.500	186.52	0.892	100.41
0.892	99.87	0.514	189.40	0.943	100.47
0.947	99.82	0.527	189.40		
$x = 0.15 \text{ in.}$		0.540	187.09	$x = 0.19 \text{ in.}$	
$y_0 = 0.740 \text{ in.}$		0.554	178.69	$y_0 = 0.744 \text{ in.}$	
0.054	100.60	0.568	174.91	0.274	99.75
0.108	100.41	0.581	169.69	0.328	107.54
0.162	100.41	0.595	160.93	0.341	130.61
0.216	100.30	0.608	158.00	0.355	165.90
0.270	100.42	0.622	160.05	0.362	176.37
0.324	101.49			0.368	176.37

\* Bulk velocity - 12.7 ft./sec.

Reynolds number based on channel cross section - 7,630

Reynolds number based on cylinder - 1221

Average temperature of cylinder - 310.8°F.

Rate of dissipation of thermal energy 5.41 watts/in.



Table I, Part 2 (cont'd.)

Temperature Distribution

$y/y_o$	$t_{o_F.}$	$y/y_o$	$t_{o_F.}$	$y/y_o$	$t_{o_F.}$
$x = 0.19$ in.		0.713	101.00	0.535	139.34
$y_o = 0.744$ in.		0.745	99.94	0.561	139.92
0.375	171.14	0.785	99.94	0.587	142.24
0.382	161.22	0.892	99.94	0.612	150.79
0.395	151.65	0.949	100.00	0.625	154.25
0.422	146.00	0		0.632	157.14
0.436	146.00	$x = 0.25$ in.		0.638	162.97
0.462	149.61	$y_o = 0.774$ in.		0.645	163.55
0.489	150.20	0.070	100.04	0.651	162.97
0.516	150.20	0.121	100.04	0.658	155.99
0.543	149.34	0.173	100.04	0.664	146.29
0.570	146.89	0.225	100.11	0.676	118.80
0.583	146.00	0.276	100.22	0.690	103.62
0.597	146.00	0.328	107.84	0.742	100.36
0.610	146.90	0.341	131.17	0.793	100.36
0.624	150.80	0.354	155.98	0.845	100.11
0.637	159.15	0.360	160.04	0.897	100.05
0.650	174.05	0.367	160.04	0.937	100.00
0.657	179.69	0.380	155.98		
0.664	176.09	0.406	144.56	$x = 0.35$ in.	
0.671	165.60	0.432	141.07	$y_o = 0.744$ in.	
0.677	143.39	0.457	140.05	0.247	100.35
0.691	115.00	0.483	139.34	0.301	100.95
0.704	105.73	0.509	139.34	0.355	137.59

Table I, Part 2 (cont'd.)

Temperature Distribution

$y/y_0$	$t_{o_F}$	$y/y_0$	$t_{o_F}$	$y/y_0$	$t_{o_F}$
$x = 0.35$ in.		0.206	100.11	0.656	107.89
$y_0 = 0.744$ in.		0.259	100.47	0.682	103.22
0.409	139.34	0.312	102.55	0.735	100.47
0.462	137.59	0.365	115.59	0.788	100.17
0.489	134.67	0.392	123.77	0.841	100.05
0.516	135.26	0.418	127.00	0.950	100.05
0.556	138.77	0.444	128.20	$x = 0.64$ in.	
0.570	140.50	0.444	127.00	$y_0 = 0.751$ in.	
0.583	141.08	0.458	128.06	0.094	99.94
0.597	142.24	0.471	128.20	0.148	99.94
0.610	143.40	0.471	127.59	0.201	100.41
0.624	143.40	0.484	128.20	0.254	102.02
0.637	138.75	0.497	128.70	0.308	105.03
0.650	126.40	0.497	122.89	0.362	108.97
0.677	104.03	0.511	128.06	0.414	112.12
0.731	100.11	0.524	128.20	0.467	115.00
0.785	99.94	0.524	127.89	0.521	115.29
0.839	100.17	0.550	128.77	0.574	113.39
0.892	100.04	0.550	126.40	0.627	110.56
0.941	100.00	0.577	128.19	0.680	106.15
$x = 0.45$ in.		0.603	126.12	0.734	102.31
$y_0 = 0.756$ in.		0.630	117.32	0.787	100.65
0.100	99.87	0.643	112.42	0.840	100.11
0.153	100.11				

Table I, Part 2 (cont'd.)

Temperature Distribution

$x/y_o$	$t_{oF.}$	$y/y_o$	$t_{oF.}$	$y/y_o$	$t_{oF.}$
$x = 0.64 \text{ in.}$ $y_o = 0.751 \text{ in.}$		0.948	100.18	0.469	104.86
0.894	100.00	$x = 1.85 \text{ in.}$ $y_o = 0.752 \text{ in.}$		0.548	104.92
0.949	100.00	0.043	101.18	0.628	104.62
$x = 1.05 \text{ in.}$ $y_o = 0.763 \text{ in.}$		0.122	102.14	0.708	104.56
0.056	100.23	0.202	103.32	0.788	104.22
0.109	100.66	0.282	104.62	0.867	104.04
0.161	101.60	0.362	106.09	0.946	103.32
0.214	102.85	0.442	107.03	$x = 9.43 \text{ in.}$ $y_o = 0.757 \text{ in.}$	
0.266	103.98	0.521	107.14	0.048	102.44
0.318	104.85	0.601	106.61	0.128	103.45
0.371	106.26	0.681	105.04	0.207	103.74
0.423	107.84	0.761	103.91	0.287	104.04
0.476	108.74	0.840	102.98	0.366	104.10
0.528	108.98	0.924	101.90	0.445	104.10
0.581	107.49	$x = 3.99 \text{ in.}$ $y_o = 0.753 \text{ in.}$		0.524	104.16
0.633	106.38	0.070	103.39	0.604	104.15
0.686	105.04	0.150	104.04	0.683	104.10
0.738	104.39	0.230	104.44	0.762	103.98
0.790	102.91	0.309	104.56	0.842	103.62
0.843	101.72	0.389	104.69	0.922	103.09
0.895	100.77				

Table I, Part 2 (cont'd.)

Air Speed Distribution

$y/y_0$	Air Speed (ft./sec.)	$y/y_0$	Air Speed (ft./sec.)	$y/y_0$	Air Speed (ft./sec.)
$x = 0.10$ in. $y_0 = 0.740$ in.		0.892	17.8	$x = 0.35$ in. $y_0 = 0.744$ in.	
		0.943	17.7		
0.676	26.8			0.194	17.9
0.730	25.9	$x = 0.25$ in. $y_0 = 0.774$ in.		0.247	19.5
0.784	24.8			0.355	11.8
0.838	23.9	0.070	16.2	0.409	5.47
0.892	22.9	0.121	18.9	0.462	6.00
0.947	21.1	0.173	18.5	0.570	6.98
		0.225	21.2	0.624	11.2
$x = 0.15$ in. $y_0 = 0.740$ in.		0.276	21.9	0.677	20.3
		0.328	22.8	0.731	20.0
0.054	16.9	0.380	2.47	0.785	19.1
0.108	18.3	0.432	1.90	0.839	18.4
0.216	21.3	0.483	2.56	0.892	17.1
0.270	22.5	0.535	2.26	0.941	12.5
0.324	23.4	0.587	2.30		
0.378	2.62	0.638	5.62	$x = 0.45$ in. $y_0 = 0.750$ in.	
0.432	0.815	0.690	22.8	0.100	15.9
0.486	0.794	0.742	21.2	0.153	16.2
0.595	0.937	0.793	20.1	0.206	16.6
0.649	1.88	0.845	19.2	0.259	16.6
0.730	23.6	0.897	16.5	0.365	12.6
0.784	22.8	0.937	16.0		
0.838	19.9				

Table I, Part 2 (cont'd.)

Air Speed Distribution

$y/y_o$	Air Speed (ft./sec.)	$y/y_o$	Air Speed (ft./sec.)	$y/y_o$	Air Speed (ft./sec.)
$x = 0.45$ in. $y_o = 0.750$ in.		0.574	11.5	0.790	14.8
0.418	8.71	0.627	13.3	0.843	13.8
0.471	7.43	0.680	15.5	0.948	10.9
0.524	7.24	0.840	15.9	$x = 9.43$ in. $y_o = 0.757$ in.	
0.577	8.94	0.894	14.8	0.049	8.70
0.630	13.6	0.949	8.07	0.128	12.6
0.682	16.4	$x = 1.05$ in. $y_o = 0.763$ in.		0.207	13.5
0.735	16.9	0.056	9.47	0.287	14.1
0.788	17.0	0.109	13.3	0.366	14.3
0.894	16.4	0.161	13.3	0.445	14.4
0.950	11.4	0.214	14.1	0.524	14.5
$x = 0.64$ in. $y_o = 0.751$ in.		0.266	14.4	0.604	14.5
0.094	15.6	0.318	15.6	0.683	14.4
0.148	15.9	0.371	15.0	0.762	14.0
0.201	15.4	0.423	14.2	0.842	13.5
0.254	15.4	0.476	14.2	0.922	11.4
0.308	14.7	0.528	14.1		
0.362	13.4	0.581	14.1		
0.414	11.9	0.633	14.1		
0.467	10.9	0.686	14.4		
0.521	10.7	0.738	15.0		

Table I, Part 3\*  
Temperature Distribution

$y/y_o$	$t_{°F.}$	$y/y_o$	$t_{°F.}$	$y/y_o$	$t_{°F.}$
$x = 0.22$ in. $y_o = 0.744$ in.		0.677	99.85	0.462	105.90
		0.731	99.67	0.515	105.35
0.032	99.54	0.785	99.67	0.570	106.05
0.086	99.54	0.839	99.62	0.623	106.16
0.140	99.54	0.892	99.62	0.877	100.33
0.194	99.54	0.946	99.77	0.731	99.51
0.247	99.51	0.970	99.71	0.785	99.51
0.301	99.62			0.838	99.47
0.325	107.22	$x = 0.30$ in. $y_o = 0.743$ in.		0.892	99.51
0.355	110.84	0.031	99.62	0.946	99.47
0.409	108.06	0.085	99.62	0.976	99.62
0.435	106.92	0.139	99.54		
0.489	106.31	0.192	99.51	$x = 0.41$ in. $y_o = 0.743$ in.	
0.543	106.81	0.246	99.51	0.030	99.70
0.570	108.59	0.300	99.51	0.058	99.70
0.597	110.26	0.355	101.25	0.125	99.70
0.624	108.97	0.408	106.36	0.192	99.70
0.651	100.12				

\* Bulk velocity - 24.8 ft./sec.  
Reynolds number based on channel cross section - 15,200  
Reynolds number based on cylinder - 2,285  
Average temperature of cylinder - 152.1°F.  
Rate of dissipation of thermal energy - 1.70 watts/in.

Table I, Part 3 (cont'd.)

Temperature Distribution

$y/y_o$	$t_{\text{°F.}}$	$y/y_o$	$t_{\text{°F.}}$
$x = 0.41 \text{ in.}$		0.811	99.85
$y_o = 0.743 \text{ in.}$		0.908	99.62
0.260	99.70		
0.327	100.76		
0.394	102.40		
0.462	103.34		
0.529	103.34		
0.610	102.13		
0.697	99.70		
0.764	99.67		
0.798	99.70		
0.865	99.70		
0.933	99.70		
0.970	99.70		
$x = 0.90 \text{ in.}$			
$y_o = 0.740 \text{ in.}$			
0.054	99.62		
0.149	99.92		
0.243	100.08		
0.338	100.38		
0.432	100.91		
0.527	101.06		
0.622	100.68		
0.716	99.85		

Table I. Temperature Distribution in  
the Wake of a Steel Cylinder

Part 4.\*

$y/y_0$	$t_{°F.}$	$y/y_0$	$t_{°F.}$	$y/y_0$	$t_{°F.}$
$x = 0.22$ in.		0.677	100.23	0.486	111.33
$y_0 = 0.744$ in.		0.731	99.62	0.541	111.83
0.027	99.67	0.785	99.62	0.595	113.99
0.059	99.54	0.839	99.54	0.649	106.77
0.113	99.54	0.892	99.59	0.703	99.85
0.167	99.54	0.946	99.54	0.757	99.74
0.220	99.59	0.972	99.70	0.811	99.77
0.274	99.54			0.865	99.77
0.328	100.35	$x = 0.30$ in.		0.919	99.77
0.355	119.58	$y_0 = 0.740$ in.		0.946	99.77
0.382	120.98	0.030	99.62	0.969	99.77
0.408	119.58	0.054	99.62		
0.435	116.65	0.108	99.62	$x = 0.41$ in.	
0.489	113.42	0.162	99.62	$y_0 = 0.752$ in.	
0.543	113.68	0.216	99.62	0.043	99.70
0.570	115.55	0.270	99.59	0.122	99.70
0.597	118.47	0.324	101.06	0.202	99.70
0.622	121.44	0.378	113.50	0.282	100.00
0.651	118.62	0.432	112.70	0.362	103.34

\* Bulk velocity - 24.8 ft./sec.  
Reynolds number based on channel cross section - 15,200  
Reynolds number based on cylinder - 2,285  
Average temperature of cylinder - 198.3°F.  
Rate of dissipation of thermal energy - 3.20 watts/in.



Table I, Part 4 (cont'd.)

Temperature Distribution

$y/y_o$	$t$ $^{\circ}\text{F.}$	$y/y_o$	$t$ $^{\circ}\text{F.}$
$x = 0.41 \text{ in.}$		0.965	99.70
$y_o = 0.752 \text{ in.}$			
0.441	106.77		
0.521	107.57		
0.601	104.64		
0.681	101.26		
0.761	99.70		
0.840	99.70		
0.920	99.70		
0.967	99.70		

\*  $x = 0.90 \text{ in.}$   
 $y_o = 0.737 \text{ in.}$

0.050	99.70
0.159	100.12
0.240	100.68
0.335	101.37
0.430	102.28
0.525	102.28
0.620	101.65
0.715	101.06
0.810	100.23
0.905	99.70

Table I. Temperature Distribution in the Wake of a Steel Cylinder

Part 5.\*

Temperature Distribution

$y/y_o$	$t_{o_F}$	$y/y_o$	$t_{o_F}$	$y/y_o$	$t_{o_F}$
$x = 0.10$ in.		0.300	99.75	0.489	130.87
$y_o = 0.744$ in.		0.327	102.67	0.502	130.59
0.583	140.03	0.341	123.77	0.529	130.00
0.624	139.40	0.347	137.88	0.542	129.72
0.637	156.39	0.354	146.59	0.556	130.00
0.650	156.74	0.361	145.79	0.569	129.72
0.650	156.80	0.367	141.37	0.583	129.72
0.664	120.81	0.381	132.64	0.596	129.72
0.677	101.00	0.394	130.30	0.610	130.71
0.732	100.35	0.421	130.30	0.623	133.22
0.785	100.54	0.435	130.87	0.630	137.65
0.839	100.54	0.448	131.76	0.637	142.59
0.892	100.54	0.462	130.30	0.643	147.17
0.944	100.54	0.462	130.87	0.650	140.32
$x = 0.15$ in.		0.475	130.87	0.664	109.54
$y_o = 0.743$ in.		0.475	131.17	0.731	100.05
0.192	100.05	0.489	131.29	0.838	100.05
0.300	99.81				

- \* Bulk velocity - 24.8 ft./sec.  
 Reynolds number based on channel cross section - 15,200  
 Reynolds number based on cylinder - 2,285  
 Average temperature of cylinder - 265.8°F.  
 Rate of dissipation of thermal energy - 5.43 watts/in.

Table I, Part 5 (cont'd.)

Temperature Distribution

$y/y_o$	$t_{oF.}$	$y/y_o$	$t_{oF.}$	$y/y_o$	$t_{oF.}$
$x = 0.15$ in.		0.624	129.72	0.429	122.32
$y_o = 0.743$ in.		0.637	134.97	0.457	120.82
0.939	100.05	0.644	138.46	0.484	120.59
$x = 0.19$ in.		0.650	140.62	0.511	120.59
$y_o = 0.757$ in.		0.657	138.87	0.538	120.82
0.220	100.00	0.664	117.66	0.565	121.75
0.301	100.05	0.677	101.72	0.586	123.89
0.328	104.04	0.732	100.05	0.599	124.12
0.341	121.75	0.839	99.95	0.606	124.10
0.348	132.05	0.944	99.95	0.613	124.14
0.355	139.05			0.620	124.12
0.362	140.79	$x = 0.29$ in.		0.626	123.48
0.368	138.46	$y_o = 0.747$ in.		0.633	122.62
0.382	131.18	0.185	99.75	0.640	119.69
0.409	126.39	0.294	100.35	0.647	112.81
0.436	125.24	0.321	102.73	0.660	105.80
0.463	124.95	0.334	109.26	0.674	101.60
0.489	124.65	0.348	115.46	0.728	100.12
0.516	124.95	0.362	122.04	0.837	100.00
0.543	124.95	0.375	123.18	0.931	99.94
0.556	126.72	0.389	123.48		
0.583	127.00	0.395	123.79	$x = 0.34$ in.	
0.610	128.19	0.402	123.79	$y_o = 0.744$ in.	
				0.153	100.00

.e I, Part 5 (cont'd.)

Temperature Distribution

$y/y_o$	$t_{o_F.}$	$y/y_o$	$t_{o_F.}$	$y/y_o$	$t_{o_F.}$
$x = 0.34$ in. $y_o = 0.744$ in.		0.551	112.70	0.742	102.31
0.301	101.01	0.607	110.34	0.793	100.77
0.355	107.07	0.663	101.54	0.845	100.47
0.409	115.75	0.720	101.00	0.897	100.47
0.462	117.03	0.776	100.77	0.946	100.47
0.516	117.20	0.832	100.65	$x = 0.89$ in. $y_o = 0.762$ in.	
0.570	116.85	0.888	100.54	0.055	100.60
0.624	112.87	0.944	99.87	0.108	100.77
0.677	103.39	$x = 0.58$ in. $y_o = 0.774$ in.		0.160	101.25
0.758	99.95	0.070	100.17	0.213	102.02
0.839	99.87	0.122	100.22	0.265	102.62
0.917	100.05	0.173	100.77	0.318	103.39
$x = 0.39$ in. $y_o = 0.713$ in.		0.224	101.01	0.370	104.22
0.055	100.47	0.276	102.14	0.423	104.98
0.102	100.41	0.328	103.68	0.475	105.67
0.158	100.47	0.380	105.39	0.528	105.74
0.215	100.60	0.432	107.01	0.580	105.15
0.271	101.00	0.483	108.11	0.633	104.27
0.327	103.51	0.535	107.84	0.685	103.51
0.383	110.00	0.587	106.73	0.738	102.79
0.439	113.00	0.638	104.69	0.790	102.19
0.495	113.79	0.690	103.45	0.843	101.43

Table I, Part 5 (cont'd.)

Temperature Distribution

$y/y_o$	$t_{\circ F.}$	$y/y_o$	$t_{\circ F.}$
$x = 0.89 \text{ in.}$		0.940	101.67
$y_o = 0.762 \text{ in.}$			
0.895	100.95	$x = 9.43 \text{ in.}$	
0.944	100.29	$y_o = 0.753 \text{ in.}$	
		0.044	102.38
$x = 1.69 \text{ in.}$		0.097	102.74
$y_o = 0.740 \text{ in.}$		0.150	102.79
0.027	101.29	0.203	102.86
0.081	101.67	0.256	102.92
0.135	101.96	0.310	102.92
0.189	102.20	0.363	102.98
0.243	102.79	0.416	102.86
0.297	103.15	0.469	102.92
0.351	103.80	0.522	102.92
0.406	104.27	0.575	102.86
0.460	104.50	0.628	102.86
0.514	104.62	0.681	102.86
0.568	104.44	0.734	102.86
0.622	103.92	0.788	102.79
0.676	103.39	0.841	102.74
0.730	102.97	0.894	102.67
0.784	102.55	0.950	102.20
0.838	102.25		
0.891	102.02		

Table I, Part 5 (cont'd.)

Air Speed Distribution

$y/y_0$	Air Speed (ft./sec.)	$y/y_0$	Air Speed (ft./sec.)	$y/y_0$	Air Speed (ft./sec.)
$x = 0.19$ in. $y_0 = 0.757$ in.		0.090	28.9	0.271	29.0
		0.143	29.9	0.327	28.1
0.049	31.0	0.304	34.2	0.383	24.0
0.102	30.2	0.357	26.0	0.439	20.6
0.155	31.5	0.411	16.8	0.495	19.1
0.207	31.6	0.464	17.2	0.551	20.1
0.260	36.3	0.518	17.8	0.607	24.0
0.313	35.7	0.572	16.7	0.663	26.2
0.366	9.06	0.625	21.3	0.720	28.8
0.419	9.87	0.679	34.0	0.776	28.8
0.472	10.4	0.732	33.4	0.832	27.9
0.524	9.12	0.786	32.5	0.888	27.4
0.577	9.58	0.835	31.7	0.944	26.7
0.630	16.0	0.839	31.7		
0.683	36.1	0.893	30.8	$x = 0.58$ in. $y_0 = 0.774$ in.	
0.736	35.2	0.949	28.8	0.070	25.4
0.789	34.0			0.122	27.1
0.842	31.4	$x = 0.39$ in. $y_0 = 0.713$ in.		0.173	27.8
0.897	32.4	0.055	26.1	0.224	27.8
0.952	31.4	0.102	27.4	0.276	27.5
$x = 0.29$ in. $y_0 = 0.747$ in.		0.158	28.0	0.328	26.8
0.044	27.0	0.215	28.5	0.380	25.4

Table I, Part 5 (cont'd.)

Air Speed Distribution

$y/y_0$	Air Speed (ft./sec.)	$y/y_0$	Air Speed (ft./sec.)	$y/y_0$	Air Speed (ft./sec.)
$x = 0.58$ in.		0.475	24.9	0.568	25.4
$y_0 = 0.774$ in.		0.528	25.0	0.622	25.4
0.432	24.1	0.580	25.1	0.676	25.4
0.483	23.9	0.633	25.4	0.730	25.4
0.535	23.8	0.685	25.7	0.784	25.4
0.587	24.6	0.738	25.9	0.838	25.4
0.638	26.1	0.790	25.7	0.891	24.7
0.690	27.2	0.843	25.7	0.940	23.6
0.742	28.3	0.895	25.5	$x = 9.43$ in.	
0.793	28.0	0.944	22.6	$y_0 = 0.753$ in.	
0.845	27.5	$x = 1.69$ in.		0.044	22.9
0.897	27.0	$y_0 = 0.740$ in.		0.097	24.4
0.946	24.1	0.027	22.8	0.150	24.8
$x = 0.89$ in.		0.081	24.3	0.203	25.2
$y_0 = 0.762$ in.		0.135	25.2	0.256	25.4
0.055	21.5	0.189	25.4	0.310	25.5
0.108	24.4	0.243	25.6	0.363	25.7
0.160	25.4	0.297	25.4	0.416	25.7
0.213	25.5	0.351	25.4	0.469	25.7
0.265	25.6	0.406	25.4	0.522	25.7
0.318	25.5	0.460	25.4	0.628	25.6
0.370	25.3	0.514	25.4	0.681	25.4
0.423	25.0				

Table I, Part 5 (cont'd.)

Air Speed Distribution

$y/y_0$     Air Speed  
          (ft./sec.)

$x = 9.43$  in.

$y_0 = 0.753$  in.

0.734      25.2

0.788      25.0

0.841      24.7



Table I, Part 6\*

Temperature Distribution

$y/y_o$	$t_{oF.}$	$y/y_o$	$t_{oF.}$	$y/y$	$t_{oF.}$
$x = 0.14$ in.		0.597	166.82	0.323	98.97
$y_o = 0.745$ in.		0.624	166.62	0.350	112.62
0.034	88.82	0.651	195.86	0.378	146.22
0.087	91.41	0.678	109.88	0.405	140.59
0.141	92.96	0.732	104.03	0.432	134.63
0.195	94.60	0.785	105.40	0.459	127.90
0.248	96.12	0.839	106.84	0.486	125.69
0.215	97.26	0.893	108.48	0.513	126.94
0.302	98.14	0.946	111.43	0.540	126.73
0.329	99.85	0.974	114.11	0.567	125.47
0.356	140.97			0.594	135.50
0.383	188.33	$x = 0.21$ in.		0.648	152.07
0.409	164.08	$y_o = 0.739$ in.		0.621	144.73
0.436	156.86	0.032	89.13	0.675	104.79
0.463	203.46	0.080	91.56	0.729	103.68
0.490	236.83	0.134	93.04	0.783	105.25
0.517	249.00	0.188	94.68	0.838	107.02
0.544	238.39	0.242	96.17	0.892	108.51
0.570	203.16	0.296	97.95		

\* Bulk velocity - 24.8 ft./sec.  
 Reynolds number based on channel cross section - 15,200  
 Reynolds number based on cylinder - 2,285  
 Average temperature of cylinder - 285.2°F.  
 Rate of dissipation of thermal energy - 5.42 watts/in.  
 Temperature of upper wall - 130°F.  
 Temperature of lower wall - 70°F.

Table I, Part 6 (cont'd.)

Temperature Distribution

$y/y_o$	$t_{o_F.}$	$y/y_o$	$t_{o_F.}$	$y/y_o$	$t_{o_F.}$
$x = 0.21 \text{ in.}$		0.946	110.98	0.266	100.08
$y_o = 0.739 \text{ in.}$		0.970	114.41	0.348	102.86
0.946	110.87	$x = 0.43 \text{ in.}$		0.429	104.99
0.968	112.62	$y_o = 0.746 \text{ in.}$		0.511	105.85
$x = 0.33 \text{ in.}$		0.035	88.22	0.592	105.35
$y_o = 0.740 \text{ in.}$		0.115	92.06	0.674	105.17
0.027	88.60	0.196	94.22	0.755	106.08
0.080	91.26	0.276	96.84	0.837	107.60
0.134	93.01	0.357	103.38	0.918	110.37
0.188	94.53	0.437	111.40	0.969	114.67
0.242	96.11	0.517	113.53	$x = 0.43 \text{ in.}$	
0.296	98.02	0.598	111.74	$y_o = 0.740 \text{ in.}$	
0.350	106.81	0.678	106.54	0.038	93.16
0.405	120.68	0.759	105.59	0.108	97.60
0.459	120.22	0.839	107.91	0.189	100.00
0.513	119.38	0.920	110.26	0.270	101.90
0.567	120.75	0.973	116.96	0.351	102.05
0.621	122.12	$x = 0.93 \text{ in.}$		0.432	102.81
0.675	106.69	$y_o = 0.736 \text{ in.}$		0.514	103.37
0.729	104.44	0.033	87.96	0.595	103.95
0.783	103.70	0.103	92.67	0.676	104.53
0.838	107.02	0.185	96.58	0.757	105.55
0.888	108.59				

Table I, Part 6 (cont'd.)

Temperature Distribution

$y/y_o$	$t$ $^{\circ}\text{F.}$
$x = 9.43 \text{ in.}$	
$y_o = 0.740 \text{ in.}$	
0.838	106.74
0.919	109.17
0.970	115.17

Table I, Part 6 (cont'd.)

Air Speed Distribution

$y/y_o$	Air Speed (ft./sec.)	$y/y_o$	Air Speed (ft./sec.)	$y/y_o$	Air Speed (ft./sec.)
$x = 0.14$ in.		0.296	31.06	0.350	31.95
$y_o = 0.745$ in.		0.350	33.83	0.405	23.89
0.034	19.73	0.405	2.01	0.459	24.50
0.087	22.06	0.513	2.92	0.513	32.24
0.141	24.15	0.567	2.25	0.567	22.96
0.195	25.57	0.648	9.59	0.621	24.03
0.248	27.59	0.621	1.82	0.675	28.98
0.302	30.09	0.675	36.28	0.729	27.65
0.356	26.93	0.729	32.81	0.783	25.66
0.678	29.89	0.783	31.98	0.838	25.05
0.732	28.01	0.838	31.55	0.888	24.58
0.785	25.74	0.892	30.57	0.946	24.10
0.839	24.50	0.946	28.58	0.970	21.10
0.893	23.49	0.968	29.58	$x = 0.43$ in.	
0.946	21.29	$x = 0.33$ in.		$y_o = 0.746$ in.	
0.974	18.83	$y_o = 0.740$ in.		0.035	21.26
$x = 0.21$ in.		0.027	18.63	0.115	24.63
$y_o = 0.739$ in.		0.080	20.44	0.196	25.98
0.032	21.94	0.134	21.71	0.276	27.89
0.080	23.84	0.188	22.78	0.357	28.21
0.134	25.48	0.242	23.84	0.437	26.48
0.188	27.53	0.296	31.27	0.517	25.03
0.242	28.72				

Table I, Part 6 (cont'd.)

Air Speed Distribution

$y/y_0$     Air Speed  
          (ft./sec.)

$x = 0.43$  in.

$y_0 = 0.746$  in.

0.598      25.56

0.678      26.14

0.759      23.35

0.839      22.84

0.920      21.97

0.973      12.44

$x = 0.93$  in.

$y_0 = 0.736$  in.

0.033      14.54

0.103      20.20

0.185      21.63

0.266      22.78

0.348      23.42

0.429      24.30

0.511      25.45

0.592      24.53

0.674      23.93

0.755      23.69

0.837      22.95

0.918      21.17

0.969      12.61

$y/y_0$     Air Speed  
          (ft./sec.)

$x = 9.43$  in.

$y_0 = 0.740$  in.

0.038      9.87

0.108      14.65

0.189      16.43

0.270      16.65

0.351      17.22

0.432      17.93

0.514      17.99

0.595      17.72

0.676      17.41

0.757      17.27

0.838      16.02

0.919      14.46

0.970      7.07

Table I, Part 7\*

Temperature Distribution

$y/y_o$	$t_{o_F.}$	$y/y_o$	$t_{o_F.}$	$y/y_o$	$t_{o_F.}$
$x = 0.13 \text{ in.}$		0.594	117.67	0.330	103.26
$y_o = 0.764 \text{ in.}$		0.607	119.21	0.343	106.49
0.267	99.94	0.614	119.97	0.357	110.97
0.319	100.00	0.620	121.17	0.370	113.29
0.332	103.15	0.634	119.50	0.377	114.20
0.346	112.77	0.647	108.56	0.383	114.20
0.352	117.91	0.660	101.72	0.390	114.09
0.359	120.87	0.686	99.87	0.397	113.91
0.365	121.46	0.738	99.94	0.410	113.29
0.372	120.40	0.791	99.87	0.437	111.55
0.385	117.91	0.843	99.94	0.464	111.14
0.398	117.03	0.937	99.94	0.491	111.14
0.424	115.29	0.937	99.87	0.518	111.14
0.450	114.71			0.538	111.14
0.476	114.66	$x = 0.19 \text{ in.}$		0.558	111.85
0.503	114.60	$y_o = 0.746 \text{ in.}$		0.571	112.70
0.529	114.84	0.088	99.87	0.584	113.68
0.555	115.59	0.303	100.12	0.598	113.86
0.581	116.74	0.316	100.89		

\* Bulk velocity - 44.7 ft./sec.

Reynolds number based on channel cross section - 26,900

Reynolds number based on cylinder - 4,440

Average temperature of cylinder - 206.2°F.

Rate of dissipation of thermal energy - 5.42 watts/in.

Table I, Part 7 (cont'd.)

Temperature Distribution

$y/y_o$	$t_{\circ F.}$	$y/y_o$	$t_{\circ F.}$	$y/y_o$	$t_{\circ F.}$
$x = 0.19$ in.		0.494	110.91	0.362	102.67
$y_o = 0.746$ in.		0.521	110.91	0.415	103.86
0.605	114.17	0.547	110.56	0.468	104.57
0.611	114.17	0.574	110.45	0.495	104.69
0.618	113.85	0.587	110.40	0.521	104.69
0.625	113.00	0.601	109.99	0.574	104.10
0.631	111.84	0.614	109.20	0.628	102.91
0.638	109.82	0.627	107.84	0.654	102.08
0.652	105.79	0.640	106.32	0.681	101.73
0.665	102.55	0.654	104.57	0.734	100.47
0.678	100.77	0.680	100.77	0.787	100.05
0.732	99.87	0.734	100.06	0.840	100.00
0.839	99.94	0.787	99.94	0.894	100.00
0.942	100.00	0.840	99.94	0.942	100.00
$x = 0.25$ in.		0.894	99.87	$x = 0.75$ in.	
$y_o = 0.751$ in.		0.940	99.87	$y_o = 0.755$ in.	
0.254	99.94	$x = 0.40$ in.		0.099	99.94
0.308	100.54	$y_o = 0.752$ in.		0.152	100.30
0.334	102.20	0.149	100.00	0.205	100.42
0.361	106.84	0.202	100.05	0.258	100.84
0.388	108.34	0.255	100.42	0.311	101.14
0.414	109.99	0.309	101.49	0.364	101.49
0.467	110.51				

Table I, Part 7 (cont'd.)

Temperature Distribution

$y/y_o$	$t_{\circ F.}$	$y/y_o$	$t_{\circ F.}$
$x = 0.75 \text{ in.}$		0.604	100.96
$y_o = 0.755 \text{ in.}$		0.683	100.96
0.417	102.03	0.763	100.89
0.470	102.62	0.842	100.89
0.497	102.67	0.908	100.77
0.523	102.80	0.959	100.42
0.576	102.44		
0.629	101.74		
0.682	101.31		
0.735	100.89		
0.788	100.66		
0.841	100.42		
0.894	100.18		
0.944	100.00		
$x = 9.43 \text{ in.}$			
$y_o = 0.758 \text{ in.}$			
0.050	100.71		
0.129	100.84		
0.208	100.89		
0.288	100.96		
0.367	100.96		
0.446	100.96		
0.525	100.96		



Table I, Part 7 (cont'd.)

Air Speed Distribution

$y/y_o$	Air Speed (ft./sec.)	$y/y_o$	Air Speed (ft./sec.)	$y/y_o$	Air Speed (ft./sec.)
$x = 0.13$ in.		0.142	54.8	0.254	51.2
$y_o = 0.764$ in.		0.196	57.5	0.308	51.0
0.058	30.4	0.249	59.4	0.361	44.1
0.110	52.4	0.303	59.9	0.414	37.5
0.162	55.5	0.357	43.9	0.467	36.9
0.215	57.9	0.410	31.2	0.521	37.0
0.267	60.1	0.464	31.2	0.574	37.8
0.319	64.0	0.518	32.3	0.627	40.7
0.372	13.5	0.571	28.7	0.680	51.1
0.424	14.8	0.625	37.3	0.734	51.0
0.476	18.6	0.678	58.3	0.787	50.4
0.529	15.4	0.732	57.8	0.840	49.2
0.581	12.5	0.786	55.4	0.894	47.3
0.634	35.3	0.839	53.9	0.940	45.4
0.686	64.2	0.893	52.1		
0.738	61.8	0.942	49.6	$x = 0.40$ in.	
0.791	58.8			$y_o = 0.752$ in.	
0.843	56.6	$x = 0.25$ in.		0.043	47.2
0.895	54.0	$y_o = 0.751$ in.		0.096	48.9
0.937	51.6	0.041	44.8	0.149	50.0
		0.095	47.5	0.202	49.9
$x = 0.19$ in.		0.148	48.9	0.255	49.6
$y_o = 0.746$ in.		0.201	49.9	0.309	47.0
0.088	51.7				

Table I, Part 7 (cont'd.)

Air Speed Distribution

$y/y_o$	Air Speed (ft./sec.)	$y/y_o$	Air Speed (ft./sec.)	$y/y_o$	Air Speed (ft./sec.)
$x = 0.40$ in.		0.417	45.6	0.763	47.0
$y_o = 0.752$ in.		0.470	46.3	0.842	45.4
0.362	43.7	0.523	45.7	0.908	43.2
0.415	40.2	0.576	45.8	0.959	38.7
0.468	38.6	0.629	45.1		
0.521	38.6	0.682	45.7		
0.574	40.2	0.735	47.3		
0.628	43.0	0.788	47.7		
0.681	46.0	0.841	48.1		
0.734	49.6	0.894	47.6		
0.787	50.0	0.944	44.3		
0.840	49.4				
0.894	48.8	$x = 9.43$ in.			
0.942	47.0	$y_o = 0.758$ in.			
		0.050	40.2		
$x = 0.75$ in.		0.129	43.8		
$y_o = 0.755$ in.		0.208	45.9		
0.046	41.3	0.288	46.5		
0.099	47.0	0.367	47.1		
0.152	48.4	0.446	47.1		
0.205	48.8	0.525	47.2		
0.258	48.5	0.604	47.2		
0.311	47.7	0.683	47.1		
0.364	46.3				

Table I, Part 8\*

Air Speed Distribution

$y/y_0$	Air Speed (ft./sec.)	$y/y_0$	Air Speed (ft./sec.)	$y/y_0$	Air Speed (ft./sec.)
$x = 0.14$ in.		0.115	52.1	0.603	47.1
$y_0 = 0.739$ in.		0.196	57.5	0.683	48.9
0.024	48.0	0.276	62.1	0.762	49.3
0.053	52.5	0.357	53.8	0.841	47.5
0.120	56.1	0.437	28.5	0.921	44.5
0.188	60.9	0.517	41.7	0.968	41.9
0.256	66.4	0.598	28.5		
0.323	72.4	0.678	69.9	$x = 9.43$ in.	
0.391	4.8	0.759	62.5	$y_0 = 0.738$ in.	
0.459	10.4	0.839	58.2	0.037	35.61
0.526	10.9	0.920	53.4	0.106	41.2
0.594	4.8	0.966	48.2	0.187	45.6
0.662	70.9			0.268	46.7
0.716	64.7	$x = 0.43$ in.		0.350	47.6
0.797	58.9	$y_0 = 0.756$ in.		0.512	48.1
0.865	54.8	0.047	44.1	0.593	47.8
0.932	49.6	0.127	48.0	0.675	47.3
0.969	47.0	0.206	49.6	0.756	46.4
		0.286	46.9	0.837	44.9
$x = 0.20$ in.		0.365	46.8	0.911	41.7
$y_0 = 0.746$ in.		0.444	45.9	0.970	33.3
0.034	46.6	0.524	47.8		

\* Bulk velocity - 44.7 ft./sec.  
 Reynolds number based on channel cross section - 26,900  
 Reynolds number based on cylinder - 4,440  
 No dissipated thermal energy from cylinder

Table II. Circumferential Temperature Distribution on the Surface of a Heated Brass Cylinder

Bulk Air Velocity - 14.4 ft./sec.

Position on Circumference <sup>a</sup> Degrees	Temperature °F.	Position on Circumference Degrees	Temperature °F.
1.04 watts/in.		2.45 watts/in.	
0	127.6	0	198.0
60	106.8	60	153.2
120	111.7	120	164.8
180	110.5	180	165.2
240	116.4	240	175.6
300	103.1	300	155.7
1.64 watts/in.		3.26 watts/in.	
0	172.8	0	234.1
60	127.1	60	179.7
120	134.8	120	195.6
180	134.7	180	195.2
240	142.1	240	209.2
300	128.0	300	180.5
2.04 watts/in.		3.90 watts/in.	
0	176.4	0	257.2
60	138.7	60	196.2
120	148.4	120	227.2
180	148.4	180	220.0
240	158.6	240	238.1
300	139.3	300	191.6

<sup>a</sup> Points on the circumference are designated by polar angles.  
 0° Represents the point of the trailing edge of the cylinder and  
 90° represents the upper edge of the cylinder.

Table II. Circumferential Temperature Distribution on the Surface of a Heated Brass Cylinder

Bulk Air Velocity - 23.8 ft./sec.

Position on Circumference Degrees	Temperature °F.	Position on Circumference Degrees	Temperature °F.
1.32 watts/in.		3.12 watts/in.	
0	129.6	0	199.3
60	103.7	60	146.1
120	110.8	120	165.2
180	110.1	180	163.2
240	118.0	240	179.2
300	103.2	300	145.5
1.71 watts/in.		4.08 watts/in.	
0	146.4	0	232.0
60	114.0	60	165.3
120	123.1	120	199.0
180	122.8	180	192.0
240	124.4	240	212.1
300	114.5	300	159.1
2.44 watts/in.			
0	173.6		
60	130.0		
120	144.9		
180	144.0		
240	157.2		
300	129.7		

Table III. Thermal Energy Transfer as a Function of  
Average Surface Temperature of Cylinder

Watts/lin.in. Dissipated	Average Surface Temperature °F.	Watts/lin.in. Dissipated	Average Surface Temperature °F.
Bulk Air Velocity 6.99 ft./sec.		Bulk Air Velocity 24.3 ft./sec.	
0.089	115.2	0.946	131.6
0.576	132.2	1.799	156.8
1.365	173.8	3.209	201.3
2.506	235.2	4.141	232.0
3.972	301.2	4.383	241.3
6.395	409.2		
Bulk Air Velocity 12.7 ft./sec.		Bulk Air Velocity 44.7 ft./sec.	
0.226	112.0	1.029	121.5
0.423	118.0	3.078	160.8
0.782	132.8	3.882	176.3
1.815	174.8	4.275	195.3
3.347	238.8	6.147	220.8
4.238	263.4	7.489	244.2
5.354	312.0		
6.771	363.6		

Table IV. Eddy Conductivity and Eddy Viscosity in the Wake of a Heated Cylinder

$y/y_o^a$	$\epsilon_{cy}^b$ ft. <sup>2</sup> /sec.	$\epsilon_{my}^c$ ft. <sup>2</sup> /sec.	$\frac{\epsilon_{my}}{\epsilon_{cy}}$
-----------	---	---	---------------------------------------

$x^d = 0.72$  in.  
Bulk Velocity - 6.99 ft./sec.

0.52	0.0075	0.0375	5.00
0.54	0.0066	0.0259	3.92
0.56	0.0082	0.0232	2.83
0.58	0.0117	0.0183	1.56
0.60	0.0146	0.0150	1.03
0.62	0.0179	0.0122	0.68
0.64	0.0211	0.0086	0.41
0.66	0.0204	0.0100	0.49
0.68	0.0193	0.0079	0.41
0.70	0.0196	0.0049	0.25

$x = 0.58$  in.  
Bulk Velocity - 24.8 ft./sec.

0.52	0.0463	0.0598	1.29
0.54	0.0500	0.0778	1.55
0.56	0.0510	0.0719	1.41
0.58	0.0527	0.0553	1.05
0.60	0.0554	0.0507	0.92
0.62	0.0618	0.0495	0.80
0.64	0.0664	0.0512	0.77
0.66	0.0707	0.0623	0.88
0.68	0.0821	0.0575	0.70
0.70	0.0958	0.0629	0.657

- a Fraction of distance between walls.  
b Eddy Conductivity  
c Eddy Viscosity  
d Distance downstream from centerline of cylinder

Table V. Theoretical Correlations of Temperature and Velocity Distribution in the Wake of a Heated Cylinder

$\frac{y'}{y_b}^a$	$\frac{t-t_o}{t_c-t_o}^b$	$\frac{y'}{y_b}$	$\frac{t-t_o}{t_c-t_o}$	$\frac{y'}{y_b}$	$\frac{t-t_o}{t_c-t_o}$
Bulk Velocity 6.99 ft./sec.		$x = 1.29$ in.		0.727	0.077
$x^c = 0.72$ in.		0	1.000	0.770	0.051
0	1.000	0.043	0.988	0.812	0.038
0.058	0.980	0.085	0.884	1.000	0
0.117	0.920	0.128	0.884	Bulk Velocity 12.7 ft./sec.	
0.175	0.894	0.171	0.789		
0.233	0.772	0.214	0.686	$x = 0.64$ in.	
0.292	0.680	0.257	0.609	0	1.000
0.350	0.580	0.299	0.532	0.050	0.997
0.408	0.484	0.342	0.474	0.100	0.972
0.467	0.384	0.385	0.417	0.149	0.926
0.525	0.284	0.427	0.359	0.199	0.860
0.583	0.200	0.470	0.308	0.249	0.789
0.641	0.124	0.513	0.256	0.299	0.704
0.700	0.068	0.555	0.218	0.349	0.612
0.817	0.012	0.598	0.180	0.399	0.515
0.933	0.004	0.641	0.135	0.449	0.410
1.000	0	0.684	0.103	0.499	0.306

<sup>a</sup> Fraction of width of wake

<sup>b</sup>  $t$  is temperature at point °F.

$t_o$  is temperature of undisturbed stream °F.

$t_c$  is temperature at center of wake °F.

<sup>c</sup> Distance downstream from centerline of cylinder



Table V. (cont'd.)

$\frac{y'}{y_b}$	$\frac{t-t_0}{t_c-t_0}$	$\frac{y'}{y_b}$	$\frac{t-t_0}{t_c-t_0}$	$\frac{y'}{y_b}$	$\frac{t-t_0}{t_c-t_0}$
Bulk Velocity 12.7 ft./sec.		0.343	0.571	0.105	0.959
$x = 0.64$ in.		0.381	0.516	0.158	0.910
0.549	0.202	0.419	0.450	0.211	0.843
0.599	0.137	0.457	0.385	0.264	0.767
0.648	0.085	0.495	0.341	0.316	0.683
0.698	0.052	0.534	0.297	0.369	0.600
0.748	0.033	0.571	0.242	0.421	0.521
0.798	0.020	0.610	0.198	0.474	0.446
0.848	0.013	0.648	0.154	0.526	0.381
0.898	0.007	0.686	0.121	0.579	0.319
0.948	0.007	0.724	0.088	0.631	0.262
1.000	0	0.763	0.066	0.685	0.215
$x = 1.05$ in.		0.800	0.044	0.736	0.173
0	1.000	0.839	0.033	0.789	0.151
0.038	0.989	0.876	0.022	0.841	0.109
0.076	0.967	0.915	0.011	0.895	0.085
0.114	0.912	0.953	0.011	0.947	0.063
0.152	0.857	1.000	0	1.000	0
0.191	0.802	Bulk Velocity 24.8 ft./sec.		$x = 0.89$ in.	
0.229	0.747	$x = 0.58$ in.		0	1.000
0.267	0.692	0	1.000	0.042	0.996
0.305	0.626	0.053	0.990	0.083	0.975

Table V. (cont'd.)

$\frac{y'}{y_b}$	$\frac{t-t_o}{t_c-t_o}$	$\frac{y'}{y_b}$	$\frac{t-t_o}{t_c-t_o}$
Bulk Velocity 24.8 ft./sec.		0.959	0.052
$x = 0.89$ in.		1.000	0
0.125	0.941	Bulk Velocity 44.7 ft./sec.	
0.167	0.889	$x = 0.75$ in.	
0.208	0.834	0	1.000
0.250	0.780	0.068	0.983
0.292	0.729	0.136	0.912
0.334	0.679	0.205	0.790
0.375	0.626	0.273	0.660
0.416	0.579	0.341	0.547
0.459	0.531	0.409	0.460
0.500	0.485	0.477	0.386
0.541	0.441	0.545	0.316
0.584	0.394	0.614	0.259
0.625	0.351	0.681	0.190
0.666	0.306	0.750	0.158
0.709	0.265	0.818	0.112
0.750	0.226	0.885	0.067
0.791	0.188	0.955	0.025
0.834	0.153	1.000	0
0.826	0.086		
0.918	0.064		

Table V. (cont'd.)

$\frac{y'}{y_b}$	$\frac{t-t_o}{t_c-t_o}$	$\frac{u_b-u^a}{u_b-u_c}$	$\frac{y'}{y_b}$	$\frac{t-t_o}{t_c-t_o}$	$\frac{u_b-u}{u_b-u_c}$
Bulk Velocity - 44.7 ft./sec.			1.000	0	0
x = 0.19 in.			x = 0.25 in.		
0	1.000	1.000	0	1.000	1.000
0.048	1.002	1.020	0.083	0.999	0.994
0.096	1.005	1.060	0.166	0.993	0.981
0.144	1.010	1.104	0.249	0.989	0.956
0.191	1.015	1.14	0.332	0.967	0.939
0.239	1.040	1.180	0.415	0.921	0.895
0.287	1.081	1.200	0.498	0.784	0.814
0.335	1.140	1.210	0.581	0.575	0.546
0.383	1.200	1.185	0.664	0.345	0.273
0.431	1.240	1.140	0.746	0.092	0.099
0.479	1.270	1.084	0.830	0.032	0.044
0.526	1.276	1.000	0.914	0.013	0.012
0.574	1.240	0.907	1.000	0	0
0.622	1.085	0.806	x = 0.40 in.		
0.670	0.855	0.657	0	1.000	1.000
0.719	0.569	0.424	0.064	0.996	0.993
0.766	0.324	0.182	0.129	0.970	0.954
0.814	0.162	0.040	0.193	0.921	0.897

<sup>a</sup>  $u_b$  is velocity at edge of wake ft./sec.  
 $u$  is velocity at point ft./sec.  
 $u_c$  is velocity at center of wake ft./sec.

Table V. (cont'd.)

$\frac{y'}{y_b'}$	$\frac{t-t_o}{t_c-t_o}$	$\frac{u_b-u}{u_b-u_c}$
x = 0.40 in.		
0.257	0.849	0.834
0.321	0.763	0.746
0.386	0.659	0.659
0.450	0.547	0.571
0.514	0.429	0.484
0.579	0.331	0.389
0.642	0.238	0.278
0.706	0.155	0.167
0.771	0.088	0.111
0.835	0.045	0.072
1.000	0	0

Propositions Submitted by David Malcolm Mason, Jr.

Ph. D. Oral Examination, May 25, 1949, 1:15 P. M., Crellin Conference Room.

Committee: Professor Sage (Chairman), Professors P. Kyropoulos, Lacey, Lindvall, Pauling, Swift, and Yost.

---

Chemical Engineering

1. Analysis shows that flame velocities in  $\text{CO-O}_2\text{-H}_2\text{O}$  mixtures measured by the soap bubble method (1) correlate as a function of the H-atom concentration present. This fact substantiates the independent results based on the Bunsen burner method of determining flame velocities (2).

2. The temperature and velocity distribution in the wake of a heated cylinder conforms to Prandtl's momentum transfer theory of turbulence and not to Taylor's vorticity transfer theory (3).

3. In textbooks the derivation of equations of heat conduction in moving fluids is often based on an energy balance where the only forms of energy considered are heat and internal energy. Thus it is tacitly assumed that the other forms of energy are negligible, but such an assumption is invalid in certain cases.

4. Most of the empirical data on the velocity distribution existing in the Karman vortex system in the wake of an obstacle (4) are not accurate due to errors in simple hot wire anemometer measurements of velocity fluctuations of high frequency and large amplitudes. It is suggested that accurate measurements of velocity distribution in the Karman vortex system be obtained by means of recently developed modified hot wire anemometer circuits (5).

5. The width of the wake of a heated cylinder is found empirically to be proportional to the square root of the distance downstream from the cylinder. This experimental fact confirms the relationship predicted by dimensional analysis (6) and illustrates the utility of dimensional analysis in solving physical problems.

Mechanical Engineering

1. At high compression ratios the discrepancy between the actual and calculated curves of thermal efficiency versus compression ratio for an internal combustion engine is reported as not being understood (7). One effect that has not been considered is the deviation of the compressibility factor of the gases from unity at high compression ratios, and when taken into account this effect reduces the discrepancy.

2. It is suggested that the standard practice of reporting the coefficient of performance and other properties of refrigerants for one standard evaporator temperature ( $50^\circ\text{F}$ ) be supplanted by presenting

the data over a wide range of evaporator temperatures. Then the relative performance of different refrigerants at actual operating evaporator temperatures will be evident.

3. In fluid dynamics research with moist air as the working substance, there is a need for accurate experimental measurements of the viscosity of the gaseous mixture at different temperatures as a function of water vapor content. Uncertainty exists in data calculated from theoretical equations (8), and the empirical data reported in the literature are scarce and inconsistent (9).

### Chemistry

1. The rate of decomposition of sodium dithionite in the absence of oxygen in aqueous solutions is first order with respect to dithionite and not second order as reported in the literature (10).

2. Bisulfite ion catalyzes the decomposition of sodium dithionite in the absence of oxygen in aqueous solutions, and the reaction rate is independent of the sulfite or hydrogen ion concentration in buffered sulfurous acid solutions.

-----

1. Stevens, F. W., NACA Tech. Rept. No. 176 (1923)
2. Tanford, C. and Pease, R. N., J. Chem. Phys., 15, 431-433, (1947)
3. Taylor, G. I., Proc. Roy. Soc., London, A135, 685-701, (1932)
4. Fage, A. and Johansen, F. C., Proc. Roy. Soc., London, A116, 170-197, (1927)
5. Mock, W. C., Jr. and Dryden, H. L., NACA Tech. Rept. No. 448, (1933)
6. Goldstein, S., Modern Developments in Fluid Dynamics, II, Oxford University Press, (1938)
7. Campbell, J. K., et al, SAE Bulletin No. 221, (1948)
8. Chapman, S. and Cowling, T. G., Mathematical Theory of Non-Uniform Gases, Cambridge University Press, (1939)
9. International Critical Tables, Vol. V, (1929)
10. Jellinek, K., Z. phys. Chem., 93, 325, (1919)